PERGAMON

Vision Research 39 (1999) 1143–1170

Vision Research

Horizontal and vertical disparity, eye position, and stereoscopic slant perception

Benjamin T. Backus [a], Martin S. Banks [a,b,*], Raymond van Ee [a,c], James A. Crowell [d]

[a] *School of Optometry, University of California, Berkeley, CA 94720-2020, USA*
[b] *Department of Psychology, University of California, Berkeley, CA 94720-2020, USA*
[c] *Helmholtz Institute, The Netherlands*
[d] *Division of Biology, California Institute of Technology, Pasadena, CA 91125, USA*

Received 19 November 1997; received in revised form 16 March 1998

Abstract

The slant of a stereoscopically defined surface cannot be determined solely from horizontal disparities or from derived quantities such as horizontal size ratio (HSR). There are four other signals that, in combination with horizontal disparity, could in principle allow an unambiguous estimate of slant: the vergence and version of the eyes, the vertical size ratio (VSR), and the horizontal gradient of VSR. Another useful signal is provided by perspective slant cues. The determination of perceived slant can be modeled as a weighted combination of three estimates based on those signals: a perspective estimate, a stereoscopic estimate based on HSR and VSR, and a stereoscopic estimate based on HSR and sensed eye position. In a series of experiments, we examined human observers' use of the two stereoscopic means of estimation. Perspective cues were rendered uninformative. We found that VSR and sensed eye position are both used to interpret the measured horizontal disparities. When the two are placed in conflict, the visual system usually gives more weight to VSR. However, when VSR is made difficult to measure by using short stimuli or stimuli composed of vertical lines, the visual system relies on sensed eye position. A model in which the observer's slant estimate is a weighted average of the slant estimate based on HSR and VSR and the one based on HSR and eye position accounted well for the data. The weights varied across viewing conditions because the informativeness of the signals they employ vary from one situation to another.

Keywords: Stereopsis; Binocular vision; Eye movements; Induced effect; Slant perception

1. Introduction

The problem of visual space perception is the recovery of the location, shape, size, and orientation of objects in the environment from the pattern of light reaching the eyes. The visual system uses spatial differences in the two eyes' retinal images to glean information about the three-dimensional layout of the environment and this is called stereoscopic vision. Here we ask how stereoscopic information is used to recover the orientation of a planar surface; specifically we ask how the visual system determines the slant of an isolated surface that is rotated about a vertical axis. This problem is interesting because the pattern of differences in the two retinal images depends not only on a surface's slant, but also on its location with respect to the head (Ogle, 1950).

Fig. 1 depicts the geometry for binocular viewing of a vertical planar surface. The cyclopean line of sight is the line from the midpoint between the eyes to the middle of the surface patch of interest. The objective gaze-normal surface is the plane perpendicular to the cyclopean line of sight. The slant is the angle by which the surface of interest is rotated about a vertical axis from the objective gaze-normal surface (the angle S; Stevens, 1983).

What signals are available for the estimation of slant? One important signal is horizontal disparity. For a smooth surface slanted about a vertical axis, the horizontal disparity pattern can be represented locally as a horizontal size ratio (HSR), the ratio of the horizontal

* Corresponding author. Fax: +1 510 6435109; e-mail: marty@john.berkeley.edu

0042-6989/99/$ - see front matter
PII: S0042-6989(98)00139-4

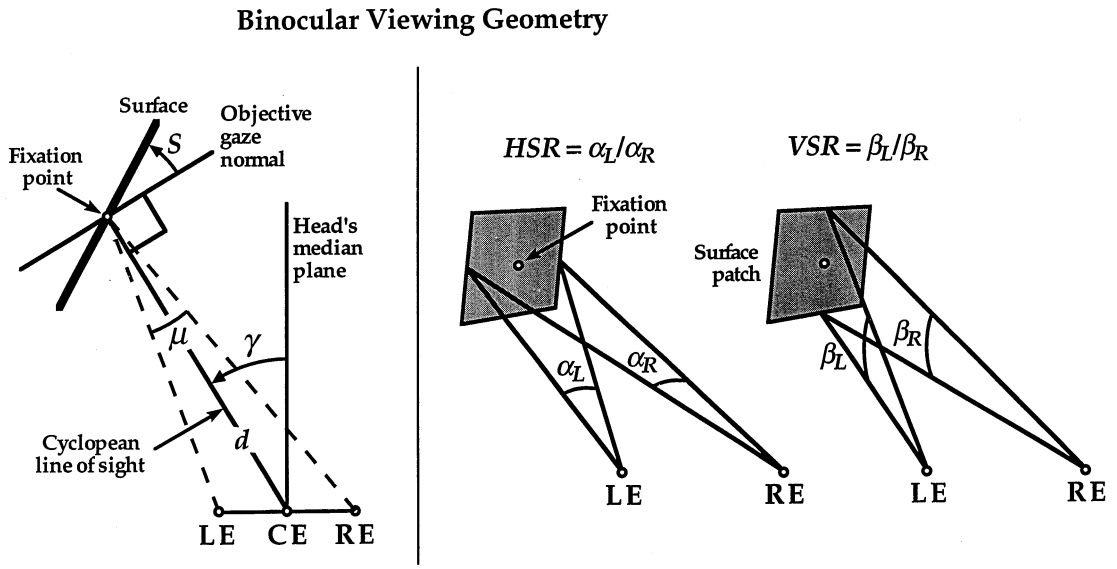

Fig. 1. Binocular viewing geometry. The left panel is an overhead (plan) view of the situation under consideration here. LE and RE refer to the left and right eyes. CE is the cyclopean eye, positioned at the midpoint between the left and right eyes. The head's median plane is the plane passing through the cyclopean eye and perpendicular to the interocular axis. A surface is fixated by the two eyes at the fixation point. The lines of sight from the two eyes are represented by the dashed lines. The cyclopean line of sight is the diagonal solid line. The distance d to the fixation point is measured along the cyclopean line of sight. The slant S is the angle between the surface and the objective gaze-normal plane (a plane perpendicular to the cyclopean line of sight); this angle is signed but otherwise equal to slant as defined by Stevens (1983). The angles γ and μ are the eyes' version and vergence, respectively. Positive slant (S) and positive azimuth (γ) are defined counterclockwise viewed from above. The right panel is an oblique view from behind the observer. The fixation point on the surface patch is indicated by the small white circle. Angles α_L and α_R are the horizontal angles subtended by the patch at the left and right eyes. The horizontal size ratio (HSR) is defined as α_L/α_R. Angles β_L and β_R are the vertical angles subtended by the surface patch. The vertical size ratio (VSR) is defined as β_L/β_R.

angles the patch subtends in the left and right eyes, respectively (α_L and α_R in Fig. 1; Rogers and Bradshaw (1993))[1]. Changes in HSR produce obvious and immediate changes in perceived slant—an increase in HSR is perceived as a clockwise rotation of the surface—so this signal must be involved in slant estimation. However, HSR by itself is ambiguous (von Helmholtz, 1962). To illustrate the ambiguity, Fig. 2 shows several surface patches in front of the observer that give rise to HSRs of 1, 1.04, and 1.08. For each value of HSR, there is an infinitude of possible slants depending on the surface's location in front of the observer. Clearly, the measurement of HSR alone does not allow an unambiguous estimate of the surface's orientation nor do any other descriptions of horizontal disparity (Longuet-Higgins, 1982a). The main purpose of the work presented here is to ascertain the other signals that, in combination with horizontal disparity, are used by the visual system to determine surface slant.

Another potentially useful signal is vertical disparity which can be represented by the vertical size ratio (VSR), the ratio of vertical angles subtended by a surface patch in the left and right eyes (β_L and β_R in Fig. 1). VSR varies with the location of a surface patch relative to the head, but does not vary with surface slant (Gillam and Lawergren, 1983). The gray circles in Fig. 3 show the VSR at various locations in the visual plane.

Another signal, also given by vertical disparity, is the rate of change in VSR with azimuth, or $\partial \mathrm{VSR}/\partial\gamma$. Fig. 3 contains pairs of surfaces at two positions in front of the observer. Notice that $\partial \mathrm{VSR}/\partial\gamma$ depends on distance (it decreases in magnitude as the iso-VSR circles diverge from one another with increasing distance), on azimuth, and on surface slant. Fig. 4 shows quantitatively how $\partial \mathrm{VSR}/\partial\gamma$ varies with distance, location, and slant.

Other useful signals are provided by the sensed positions of the eyes. Ignoring torsion, each eye has one degree of freedom in the visual plane. We can, therefore, represent eye position by two values γ and μ, which are the version and vergence angles of the eyes, respectively (Fig. 1). Fig. 5 displays the values of γ and μ at various positions in front of the observer.

Finally, useful slant information can be gleaned from non-stereoscopic perspective signals such as the texture gradient created by projection onto the retinae of sur-

[1] Our choice of signals is based on their utility for expressing disparity information in the retinal images, not on a presumption that the brain represents these quantities *per se*. Other quantities could be used (Frisby, 1984; Gårding et al., 1995; Koenderink and van Doorn, 1976; Longuet-Higgins, 1982a; Mayhew and Longuet-Higgins, 1982) without loss of generality. For planar surfaces, HSR and VSR have the virtue of being nearly independent of the size of the patch across which they are measured, even for patches up to 30° in diameter.

faces with statistically regular textures (Stevens, 1981; Cutting and Millard, 1984; Gillam and Ryan, 1992; Buckley and Frisby, 1993; Cumming et al., 1993).

We next examine how an unambiguous estimate of slant could be obtained from various combinations of the above-mentioned signals.

The slant of a vertical surface in the visual plane is related to μ, HSR, and VSR in the following way (Banks and Backus, 1998; see Appendix for derivation):

$$S \approx -\tan^{-1}\left(\frac{1}{\mu}\ln\frac{\mathrm{HSR}}{\mathrm{VSR}}\right) \quad (1)$$

In the terminology of Gårding et al. (1995), μ 'normalizes' the slant (scales HSR for changes due to viewing distance) and VSR 'corrects' the slant (corrects HSR for changes due to azimuth).

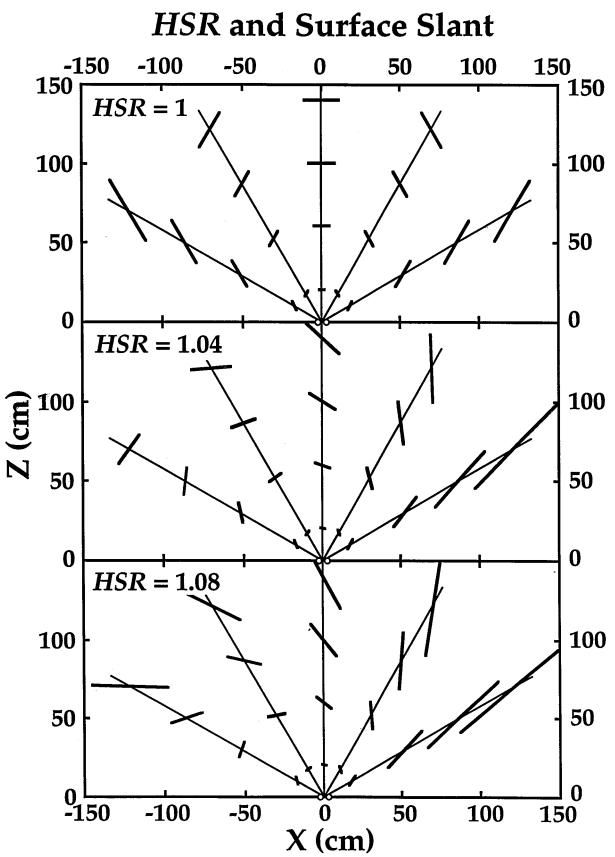

Fig. 2. HSR, position, and slant. Each panel is an overhead view of surface patches that give rise to a particular value for the horizontal size ratio (HSR). The X- and Z-axes are defined relative to the head and represent lateral and forward position (in cm) with respect to the cyclopean eye which is at the origin. The small circles near the origin represent the two eyes. The thin lines emanating from the origin correspond clockwise to azimuths of 60, 30, 0, −30, and −60°. The upper, middle, and lower panels show patches for which HSR = 1, 1.04, and 1.08, respectively. Notice that many surface slants are consistent with a given HSR depending on the patch's position relative to the head. For this reason, position and HSR uniquely specify slant, but HSR alone does not.

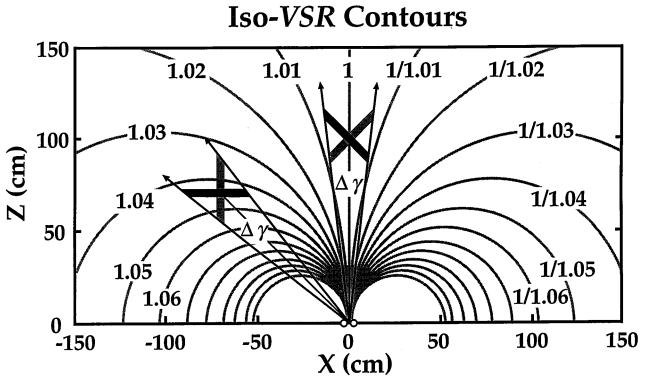

Fig. 3. VSR in the visual plane, and rate of change in VSR for different surfaces. The figure is an overhead view through the visual plane, showing the circular contours for which the vertical size ratio (VSR) is constant (gray circles). Each iso-VSR contour is labeled with its VSR value (adapted from Gillam and Lawergren, 1983). Four surface patches are shown; they have slants of ±45° at azimuths of 45 and 0°. The rate of change of VSR with respect to azimuth ($\partial\mathrm{VSR}/\partial\gamma$) can be discerned from the number of iso-VSR contours crossed by the surface patches. For patches presented eccentrically (azimuth = 45°), $\partial\mathrm{VSR}/\partial\gamma$ is quite dependent on slant; specifically, when the slant is 45° (gray bar), several iso-VSR contours are crossed whereas when the slant is −45° (black bar), few contours are crossed. For patches presented straight ahead (azimuth = 0°), $\partial\mathrm{VSR}/\partial\gamma$ does not depend on surface slant which is illustrated by the fact that both surfaces cross the same number of iso-VSR contours. The effect of distance can be discerned, too: $\partial\mathrm{VSR}/\partial\gamma$ decreases with distance in forward or eccentric gaze because the iso-VSR contours diverge with increasing distance more rapidly than do the sides of the angle $\Delta\gamma$.

Eq. (1) shows that the eyes' vergence and VSR can be used together to estimate slant from HSR. Notice from Fig. 3 and Fig. 5 that μ and VSR uniquely specify a location in the visual plane and, therefore, the combination of μ, VSR, and HSR uniquely specifies the slant and location of the surface patch.

Thus, certain subsets of signals allow unambiguous estimation of slant and we summarize them in terms of three calculations (Banks and Backus, 1998): (1) slant estimation from HSR and eye position, (2) slant estimation from HSR and VSR, and (3) slant estimation from nonstereoscopic cues such as perspective.

1.1. Slant from HSR and eye position

Slant can in principle be estimated from HSR and sensed eye position (Ogle, 1950)[2]. The natural log of VSR in Eq. (1) can be approximated by the quantity μ tan γ, yielding:

$$S \approx -\tan^{-1}\left(\frac{1}{\mu}\ln\mathrm{HSR} - \tan\gamma\right) \quad (2)$$

[2] Other instances in which horizontal disparity is interpreted using sensed eye position are discussed by Cumming et al., 1991; Collett et al., 1991; Sobel and Collett, 1991; Foley, 1980.

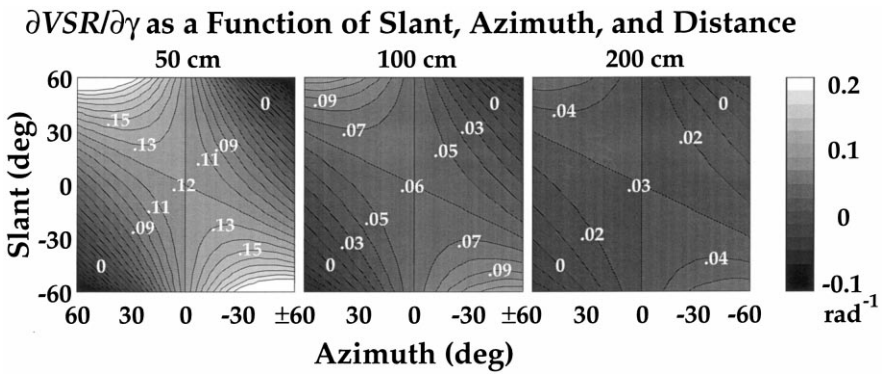

Fig. 4. $\partial VSR/\partial\gamma$ as a function of slant, azimuth, and distance. Each panel shows the values of $\partial VSR/\partial\gamma$ as a function of azimuth (abscissa) and surface slant (ordinate). Positive azimuth is plotted on the left because it corresponds to surfaces that are in leftward gaze. The three panels show, from left to right, $\partial VSR/\partial\gamma$ for distances of 50, 100, and 200 cm (where distance refers to the radial distance from the cyclopean eye to the surface patch's center). The gray bar on the right shows the relationship between gray level and the value of $\partial VSR/\partial\gamma$; the units are inverse radians. In forward gaze (azimuth = 0°), $\partial VSR/\partial\gamma$ varies with distance, but not with slant. In eccentric gaze, it varies with distance and slant. In the calculations of $\partial VSR/\partial\gamma$, we assumed an interocular distance of 6.0 cm.

where, as before, μ and γ are the vergence and version of the eyes, respectively. Note that the estimates of μ and γ (which we will call $\hat{\mu}$ and $\hat{\gamma}$) are presumably derived from extra-retinal, eye-position signals, probably of efference-copy origin (Clark and Horch, 1986).

The use of this method is schematized in Fig. 5 which displays contours of constant μ and γ. Notice that μ and γ specify a location in the visual plane and, therefore, μ, γ, and HSR uniquely determine the slant and location of the surface patch. There is some evidence that sensed eye position can be used in estimating slant

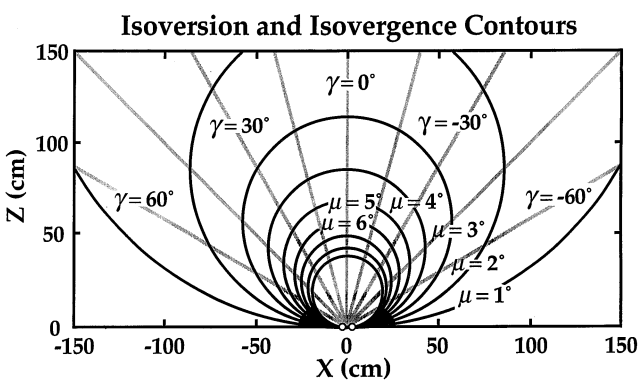

Fig. 5. Values of γ and μ in the visual plane. This is an overhead view showing the contours for which the eyes' vergence (μ) and version (γ) are constant. The iso-vergence contours are the black circles and the iso-version contours are the gray lines. The former are Vieth-Müller Circles. By the conventional definition of version (the average of the two eyes' rotations; Howard and Rogers, 1995), iso-version contours are Hyperbolae of Hillebrand rather than lines. However, we have defined version (γ) as the angle between the head's median plane and the cyclopean line of sight (Fig. 1), and by this definition, the iso-version contours are lines. Together γ and μ determine the point of fixation within the visual plane. They can be estimated from extra-retinal, eye-position signals. Together, estimates of HSR, γ and μ ($\hat{\text{HSR}}$, $\hat{\gamma}$ and $\hat{\mu}$) allow an unambiguous estimate of surface slant (see Eq. (2)).

(Amigo, 1967; Ebenholtz and Paap, 1973; Herzau and Ogle, 1937).

1.2. Slant from HSR and VSR

Slant can also be estimated from retinal-image information alone; specifically, it can be estimated from HSR, VSR, and $\partial VSR/\partial\gamma$ (Frisby, 1984; Gårding et al., 1995; Gillam and Lawergren, 1983; Koenderink and van Doorn, 1976; Longuet-Higgins, 1982a; Mayhew, 1982; Mayhew and Longuet-Higgins, 1982). The quantity μ in Eq. (1) can be replaced by $\tilde{\mu}$:

$$S \approx -\tan^{-1}\left(\frac{1}{\tilde{\mu}}\ln\frac{\text{HSR}}{\text{VSR}}\right) \tag{3}$$

where

$$\tilde{\mu} \approx \frac{1}{2}\left(\frac{\partial \text{VSR}}{\partial\gamma} + \sqrt{(\partial \text{VSR}/\partial\gamma)^2 + 4\ln(\text{VSR})\ln(\text{HSR}/\text{VSR})}\right) \tag{4}$$

One cannot illustrate this method of estimating slant in the format of Fig. 5, but the special case of rotating the surface until it appears to be gaze normal has a simple graphical interpretation. For a gaze-normal plane, $S = 0$, so by Eq. (3), HSR = VSR (Ogle, 1950; Howard and Rogers, 1995). Fig. 6 shows the surface patches for which HSR = 1.04 along with the circle for which VSR = 1.04. The intersection of these two constraints yields a series of gaze-normal surfaces at different distances and azimuths. Thus, an observer could in principle set a planar surface to gaze normal by adjusting its slant until $\hat{\text{HSR}} = \hat{\text{VSR}}$ (where $\hat{\text{HSR}}$ and $\hat{\text{VSR}}$ are the visual system's estimates of HSR and VSR). It is worth noting that this particular task can be done using $\hat{\text{HSR}}$ and $\hat{\text{VSR}}$ alone; errors in $\hat{\tilde{\mu}}$ (Eq. (3)) should have no effect.

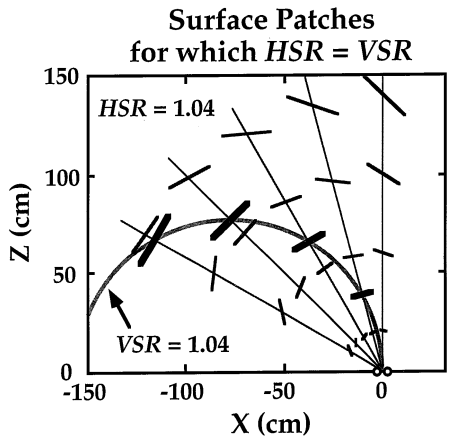

Fig. 6. Surfaces for which HSR = VSR are gaze normal. This is an overhead view showing a variety of surface patches for which HSR = 1.04 and the contour along which VSR = 1.04. The thick black segments represent the patches for which HSR = VSR = 1.04. Notice that each of those patches is perpendicular to its cyclopean line of sight (the line from the cyclopean eye to the center of the patch); the patches are gaze normal.

The visual system could estimate μ from sensed eye position ($\hat{\mu}$) and the retinal images ($\hat{\tilde{\mu}}$) in combination. Then this estimate could be used in Eqs. (2) and (3). The distinction between estimation by HSR and eye position and by HSR and VSR would then be less strict than presented above. That γ appears only in Eq. (2) and VSR only in Eq. (3) is the essential distinction between these methods.

1.3. Slant from nonstereoscopic cues

Useful indications of surface slant are provided by non-stereoscopic perspective cues such as the texture gradient created by projection onto the retinae of surfaces with statistically regular textures (e.g. Rosenholtz and Malik, 1997). Such cues were commonly present in older stereoscopic work using real objects (Ogle, 1950; Amigo, 1967, 1972; Gillam et al., 1988). In more recent work employing stereoscopic computer displays, there is still generally a perspective cue that indicates that the surface is frontoparallel to the head (Banks and Backus, 1998).

The slant specified by a given texture gradient does not vary with distance or azimuth (Sedgwick, 1986). Suppose that two surfaces, at distances d and kd from the observer, have textures that are identical up to a uniform scale factor k. If the surfaces have the same slant, they will create identical retinal images and, therefore, identical texture gradients. By similar reasoning, one can show that perspective cues to slant do not depend on the azimuth of the patch; therefore, slant estimation by perspective is independent of viewing distance and azimuth. (A particular surface will give rise to equally reliable slant-from-texture cues at different distances only if the texture is spatially broadband.)

In order to examine stereoscopic means of slant estimation, we minimized perspective cues using techniques described in Section 2. The residual perspective cues (e.g. constant dot brightness) were always consistent with a slant of 0°.

1.4. Weighting of slant estimates

The slant estimates derived from these three methods generally agree under normal viewing situations. In our conceptualization, schematized in Fig. 7, the weight associated with each slant estimate is a function of its estimated reliability, and the estimated reliability is based in turn on the quality of the information present in the signals (Landy et al., 1995; Heller and Trahiotis, 1996). A number of factors influence signal reliability. For example, consider the effects of increasing the viewing distance. As distance increases, there is no effect on the information carried by the perspective signal, but the information carried by HSR is reduced because a given set of slants maps onto ever smaller ranges of HSR, and the information conveyed by VSR is reduced because a given set of azimuths maps onto ever smaller ranges of VSR. Consequently, we assume that non-stereoscopic slant estimates are weighted more heavily relative to stereoscopic slant estimates as viewing distance increases. Other factors that affect signal reliability include the texture on the surface (e.g. vertically oriented textures render VSR more difficult to measure, noisy textures render perspective more difficult, etc.), the size of the retinal image (e.g. smaller images provide a smaller area over which to estimate VSR, which should make $\hat{\text{VSR}}$ less reliable; cf Rogers and Bradshaw (1995)).

The experiments described here were designed to test whether the signals described above are used in estimating slant, and how the weights assigned to the estimates vary across viewing conditions and stimulus properties during stereoscopic slant perception.

von Helmholtz (1962), and Ogle (1950) described the ambiguity of surface reconstruction from horizontal disparity in another context. They noted that a concave, planar, or convex surface can create the same pattern of horizontal disparities depending on viewing distance. Rogers and Bradshaw (1995) examined the use of vertical disparities and sensed eye position in the perception of surface curvature and found that both cues affected perceived curvature, but that the influence of vertical disparities was relatively greater for large stimuli. Similar findings for the amount of perceived depth in a stereogram were reported by Bradshaw et al. (1996). Thus, previous work has shown that the visual system uses an extra-retinal estimate of the eyes' vergence to aid the interpretation of horizontal disparities. In the work presented here, we show that the system also uses an extra-retinal estimate of the eyes' version.

1.5. Effect of uncertainty in stereoscopic signals

Each of the five signals described above must be measured by the visual system before it can be used to estimate the properties of the viewed surface. Obviously, none can be measured with perfect precision, so it is of interest to know the consequences of erroneous measurements in each of the signals. An efficient estimator would use the signals that, given their uncertainties, would allow the most accurate slant estimate. In this section, we make the point that the effects of signal uncertainty on slant estimation are quite dependent on the viewing situation and on the uncertainty associated with the other available signals.

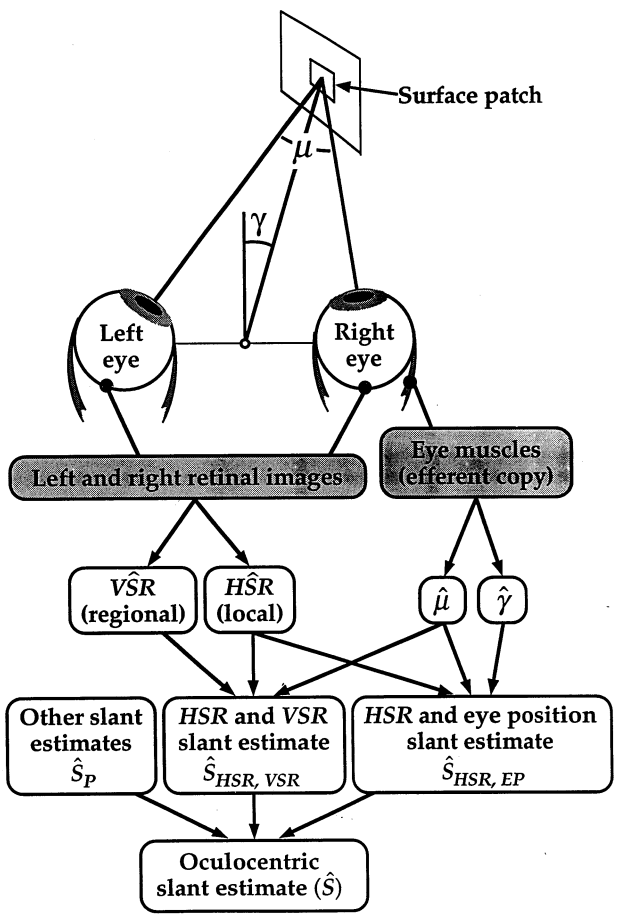

Fig. 7. Model of stereoscopic slant perception. The visual system measures five signals: HSR, VSR, and $\partial VSR/\partial\gamma$ (not shown) from the retinal images, and γ and μ from the eye muscles. It also measures signals based on other slant cues such as perspective. It combines these signals in three ways to estimate surface slant. HSR, VSR, and μ are used to estimate slant from HSR and VSR (Eq. (1)). The estimate of μ can be based either on eye position (shown), or on the retinal images ($\tilde{\mu}$, not shown; see Eqs. (3) and (4)). HSR, γ, and μ are used to estimate slant from HSR and eye position (Eq. (2)). The perspective cue signal provides the third slant estimate. The various slant estimates ($\hat{S}_{HSR,EP}$, $\hat{S}_{HSR,VSR}$ and $\hat{S}_P$) are combined in a weighted average, with the weight assigned to each slant estimate dependent on the visual system's estimate of its reliability. The final slant estimate is done in oculocentric coordinates; specifically, the computations yield an estimate of surface slant relative to the cyclopean line of sight (see Fig. 1).

Consider the consequences of error in $\hat{\mu}$ when estimating slant from HSR and eye position (Eq. (2)) or from HSR and VSR (Eq. (3)). Assume that $\hat{\mu}$ contains the same error for both means of slant estimation (as is the case if both use the more reliable of $\hat{\mu}$ and $\hat{\tilde{\mu}}$). Fig. 8 shows the error in $\hat{S}$ that results from 1° of error in $\hat{\mu}$ at a distance of 57.3 cm; the error is plotted as a function of the true slant (S) and the azimuth (γ). The left panel shows the slant errors for estimation by HSR and eye position and the right panel shows the errors for estimation by HSR and VSR. Errors in the remaining signals—$\hat{HSR}$, γ, and $\hat{VSR}$—are assumed to be zero.

Notice how different the pattern of errors is for the two means of slant estimation. The estimation errors from HSR and eye position tend toward zero when the true slant is equal to the azimuth ($S = \gamma$). This occurs because a surface whose slant is equal to its azimuth is tangent to the Vieth-Müller circle and, therefore, HSR = 1; inspection of Eq. (2) reveals that errors in $\hat{\mu}$ would not affect the slant estimate in this case[3].

The pattern of errors is quite different when slant is estimated from HSR and VSR. In this case, the estimation error is zero when $S = 0$. This occurs because HSR = VSR for gaze-normal surfaces and, from Eq. (3), an error in $\hat{\mu}$ should have no effect in this situation. Errors grow as HSR deviates from VSR. From this analysis, we conclude that an efficient slant estimator would weight the slant estimate based on HSR and eye position most heavily when $\tilde{S} \approx \hat{\gamma}$ (i.e. $\hat{HSR} \approx 1$). We also conclude that an efficient estimator would weight the estimate based on HSR and VSR most heavily when $\hat{HSR} \approx \hat{VSR}$ (or alternatively, $\hat{S} \approx 0$). Naturally, optimal weightings would also depend on the reliabilities of $\hat{HSR}$, $\hat{\gamma}$ and $\hat{VSR}$.

By similar reasoning, changes in display size ought to affect the weighting of slant estimation by HSR and VSR relative to the weighting of estimation by HSR and eye position. One should be able to measure VSR with greatest precision when the stimulus is large because VSR typically varies smoothly and systematically across the visual field (Gillam and Lawergren, 1983). Thus, the error associated with slant estimation by HSR and VSR should in principle decrease as the display is made larger. At the same time, changes in display size should not affect $\hat{\gamma}$ or $\hat{\mu}$ because these signals are measured from extra-retinal sources. Thus,

[3] When HSR = 1, Eq. (2) simplifies to $S \approx \gamma$. This relation is exact if the cyclopean eye is placed equidistant from the eyes on the Vieth-Müller circle (Gårding et al., 1995).

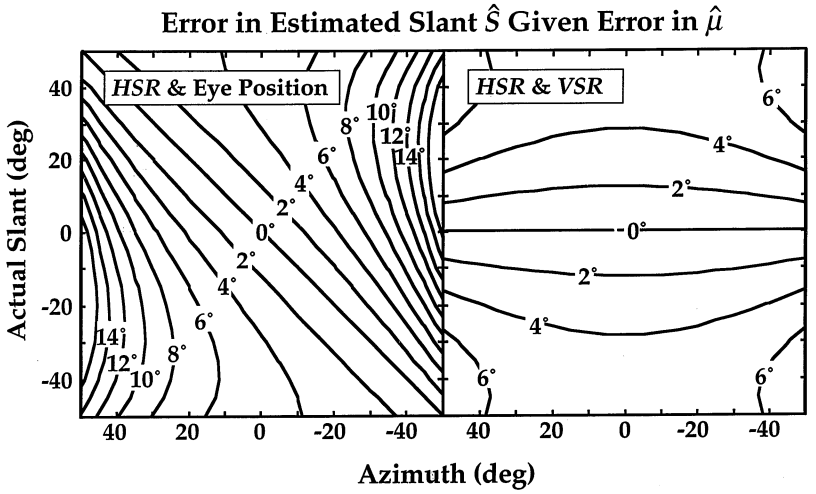

Fig. 8. Error in slant estimate due to error in the measurement of μ. The abscissa is azimuth (positive numbers to the left of the head's median plane) and the ordinate is the actual slant of the surface. The contours represent the magnitude of error in estimated slant per degree of error in $\hat{\mu}$ (in the neighborhood of $\hat{\mu} = \mu$). The left panel shows the errors when slant is estimated from HSR and eye position (Eq. (2)). The right panel shows the errors when slant is estimated from HSR and VSR (Eq. (3)). The viewing distance for these calculations was 57.3 cm (from the cyclopean eye) and the assumed interocular distance was 6.0 cm. To make these calculations, we assumed that the other signals—$\hat{\text{HSR}}$, $\hat{\gamma}$ and $\hat{\text{VSR}}$—were measured without error. Two slant estimates were calculated for each viewing condition: one for $\hat{\mu}$ 0.5° greater than the true value of μ and one for $\hat{\mu}$ 0.5° less than μ. The plotted slant error values are the differences between the two estimates.

with increasing display size, an efficient estimator would increase the weight assigned to slant estimation by HSR and VSR relative to estimation by HSR and eye position. This sort of analysis allows one to study the optimal weighting of estimates across viewing situations.

1.6. Setting slant to appear gaze normal

In our experiments, observers rotated a stereoscopic plane about a vertical axis until it appeared gaze normal. This is a somewhat special case because the computations involved are simpler than those involved in estimating slant. By way of illustration, consider Eqs. (2) and (3) above. The gaze-normal task requires the observer to rotate the surface until slant S is zero. Thus, when using HSR and eye position, $\tan^{-1}(1/\mu \ \ln\text{HSR} - \tan\gamma) \approx 0$, which implies that $\ln\text{HSR} \approx \mu \tan\gamma$. When using HSR and VSR, $\tan^{-1}(1/\tilde{\mu} \ \ln \text{HSR}/\text{VSR}) \approx 0$, or simply $\text{HSR} \approx \text{VSR}$.

It has been argued that the gaze-normal task is of limited interest and that more can be learned by asking observers to estimate non-zero surface slants (Gillam et al., 1988). There are two important justifications for using the gaze-normal task to examine the use of stereoscopic signals in slant perception. First, it is unlikely that different mechanisms underlie perception of surfaces with zero and non-zero slants. Second and most importantly, the gaze-normal task, as implemented in our experiments, allows one to isolate stereoscopic-based slant estimation from perspective-based estimation. Specifically, the residual perspective cues in our displays always indicated that the surface was gaze-normal no matter what slant was specified by the two stereoscopic means of slant estimation. Perspective cues, therefore, could not determine which of the stereoscopic means of estimation was given greater weight in a given viewing situation. For this reason, the gaze-normal task allowed us to determine the relative weights of the two stereoscopic means of slant estimation without contamination from perspective cues.

We conducted five experiments to determine the signals used in stereoscopic slant perception with particular attention to the relative weights of VSR and eye-position signals.

2. General methods

2.1. Observers

Two of the authors and a third adult (SRG), who was naive to the details of the experimental hypotheses, served as observers in all the experiments. In Experiment 4, SJF also participated; she was naive to the experimental hypotheses. In Experiment 5, co-author RVE also participated; he was an experienced psychophysical observer who at the time was familiar with the general purpose of the research, but not with the experimental details. MSB, SRG, and SJF have normal vision. BTB and RVE are myopes (-7 D, -5 D) whose vision was corrected by contact lenses. Their interocular distances are 6.2, 5.9, 6.0, 6.1, and 6.4 cm, respectively.

2.2. Apparatus

Stimuli were displayed on a haploscope consisting of two 23-in. monochrome CRT displays each seen in a mirror by one eye (Fig. 9). Each mirror and CRT were attached to an armature that rotated about a vertical axis passing through the eye's center of rotation (assumed to be 13 mm behind the corneal surface; Howard and Rogers (1995)). The face of each CRT was always perpendicular to the line of sight from the eye to the center of the screen. A small target on each screen served as the fixation aid. As the CRTs were rotated, the eyes rotated to track the targets, but the images created by the CRTs at the retinae were unchanged.

Natural pupils were used throughout. Accommodative demand of the stimulus was constant at 2.35 D (42.5 cm). Head position was fixed with a bite bar. The room was completely dark, and a black aperture occluded the frames of the monitors. Only the white dots within the display were visible.

A Macintosh 840/AV generated the stimulus and tabulated the responses. Each CRT could display 1280×1024 pixels at a refresh rate of 75 Hz. Angular subtense of a pixel was 2.5 arc min at screen center.

Despite the short viewing distance of 42.5 cm, the visual locations of the dots in our displays were specified to within ~ 30 arcsec. This high level of spatial precision was achieved by use of two procedures: anti-aliasing and spatial calibration.

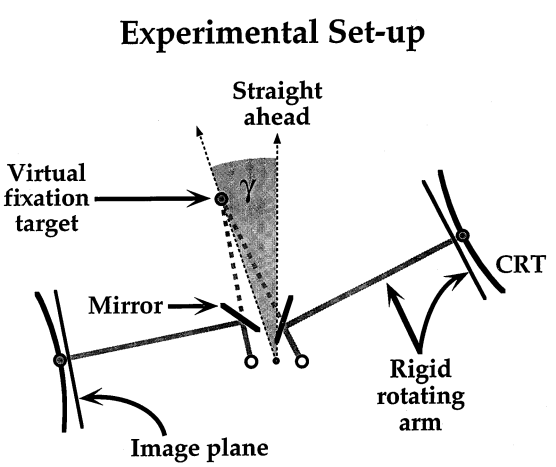

Fig. 9. Experimental apparatus. The figure is a schematic of the haploscope on which all the experiments were performed. The observer's head was fixed in position by use of a bite bar. Each eye viewed a separate CRT in a mirror. The eyes were positioned at the unfilled circles. The mirrors were rigidly attached to their respective CRTs such that each mirror and its CRT rotated together about a vertical axis that contained the center of rotation of the left or right eye. To align the axes of the haploscope pivots and the rotation centers of the eyes, we adjusted the position of the bite bar and the lateral separation between the pivot points of the two haploscope arms. Because each haploscope arm, mirror, and CRT rotated about the center of rotation of the appropriate eye, we could change the headcentric azimuth of the stimulus without altering the retinal images.

Anti-aliasing allowed dot placement at arbitrary positions between integral pixel locations. Each dot was composed of four adjacent pixels whose intensities were adjusted to place the center of brightness at the desired location taking into account the adjacent-pixel nonlinearity (Klein et al., 1996). Dot diameter was about 6 arc min; dot luminance was 10 cd/m^2 at screen center.

Spatial calibration involved the creation of a look-up table that converted desired visual directions into screen coordinates. During the calibration procedure, a mesh of thin nylon filament, stretched across a precisely milled loom, created a 36-by-26-cm grid with 1-cm spacing. The loom was mounted 1 cm in front of the CRT to be calibrated, and was viewed in the mirror from the standard viewing position. An observer positioned a dot to be coincident with specified intersections in the grid. When the dot was aligned with an intersection, its coordinates were recorded. The procedure was repeated for misaligned dots until the interpolated positions of all the dots were correct (about 70 explicit settings). The loom was removed during the experiment. Its former location defined a virtual plane onto which stimuli were projected. The calibrated area was $47 \times 35°$ on each monitor.

2.3. Stimuli

The stimuli consisted of sparse random-dot displays that minimized the use of perspective cues. The dots were placed on a simulated vertical plane; dot positions were calculated by projection through the centers of the eyes onto the virtual image planes in front of each CRT. The retinal images were, therefore, the same as would be created by a real object (except that dot size and intensity were constant). Consequently, the shape distortions that one frequently observes in stereoscopic displays were not present. The 2-dimensional shape of the simulated surface was elliptical with randomly varied height and width, so the outline shape provided no useful slant information.

Azimuth specified by eye position was manipulated by rotating the monitors about the pivots below the centers of the eyes; such rotation did not alter the retinal images. Azimuth specified by VSR was determined by the location of the simulated surface from which the images were derived. For example, a stimulus for which eye-position azimuth is 15° and VSR azimuth is $-15°$ is a surface patch that produces the retinal images of a plane to the right of the head's median plane and is viewed with the monitors positioned to the left (eyes rotated leftward).

A fixation/nonius marker was placed near the center of the displays. The true center of a slanted patch appears decentered in a monocular view. To eliminate this possible cue to slant, the plane was displaced horizontally by a random amount between $\pm °3$.

2.4. Task and procedure

The observers' task was to rotate the surface about a vertical axis until it appeared perpendicular to the line of sight (Fig. 1). Observers could perform the task easily and reliably. Initial slant was randomly chosen from values ranging from -20 to 20°. Discrete slant adjustments were made with key presses. The smallest possible adjustment (0.4°) was just noticeable on some trials; it was about half the standard deviation of 1° that was typical for slant settings. A new stimulus appeared with new dots after each press. Observers indicated when they were satisfied with a slant setting by pressing a key. They were given no feedback. A minimum of six observations was made in each condition.

To insure that observers' slant settings were unaffected by residual perspective cues in the stimuli, we conducted a monocular control experiment. The stimuli, procedure, and task were identical to those of the main experiments, but the observer (BTB) performed the task monocularly. The standard deviations of the slant settings were generally ten times greater than when he performed the task binocularly. We conclude that observers could not perform the task reliably from monocularly available cues.

3. Experiment 1: natural viewing

We first asked how well observers compensate for changes in a surface's azimuth when stereoscopic means of estimating slant agree with one another. In this natural-viewing situation, slant estimation from HSR and eye position yielded the same values as slant estimation from HSR and VSR. Nonstereoscopic cues were rendered uninformative.

3.1. Methods

The surface patch contained 300 dots. Ellipse width was chosen randomly from the uniform interval (33.1, 41.4 cm) and height was chosen from the interval (22.1, 27.6 cm). Distance specified by eye position and VSR was 57.3 cm from the midpoint of the interocular axis. Display size thus varied from $22 \times 32°$ to $27 \times 40°$.

The azimuths specified by eye position and by VSR were always equal and were -15, 0, and 15°. Observers BTB and MSB also collected data at azimuths of $\pm 7.5°$, and MSB also collected data at $\pm 3.75°$.

3.2. Results

Fig. 10 shows the results. Slant settings are plotted as a function of the eyes' version. The upper panel shows the data when slant relative to the objective gaze-normal plane is plotted (S in Fig. 1). Biases in each observer's settings have been removed by translating the data vertically until the slant setting was 0 at azimuth = 0°. If observers did not compensate for changes in the surface's azimuth, the data would lie on the solid diagonal line. If they compensated completely, the data would lie on the dashed horizontal line. The actual settings always show nearly complete compensation.

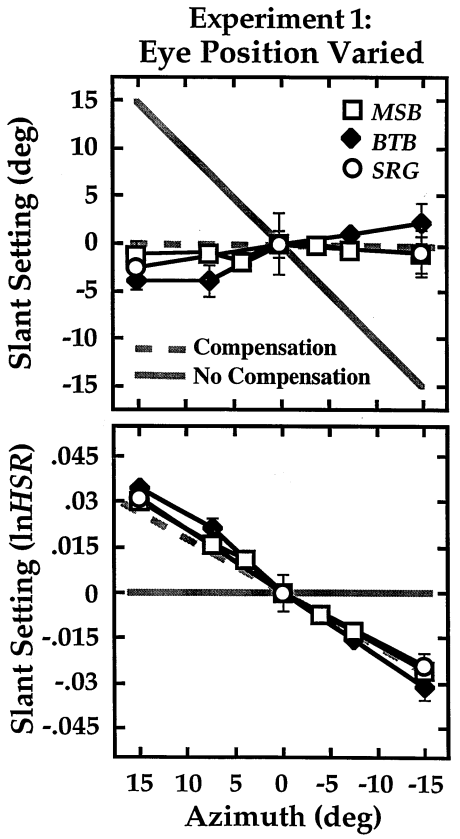

Fig. 10. Results of Experiment 1. In this 'natural viewing' experiment, eye position and VSR specified the same azimuth. Observers adjusted the slant of a stereoscopically defined plane until it appeared gaze normal. The upper panel plots each observer's average slant settings (in degrees) as a function of the azimuth of the stimulus. A value of 0° on the ordinate corresponds to the objective gaze-normal plane. The abscissa has positive values on the left because positive values correspond to leftward gaze. The dashed and solid lines represent the predicted values for complete compensation and no compensation, respectively. The lower panel plots the same data, but the slant settings have been converted to values of lnHSR in the retinal images. The dashed gray line again represents the predictions if observers compensated completely for changes in azimuth and, therefore, set the slants to the objective gaze normal; the solid line again represents no compensation. The lnHSR predictions are based on an assumed interocular distance of 6.1 cm. Error bars correspond to ± 1 standard deviation. The data for each observer have been normalized to 0° for an azimuth of 0°. The values subtracted for this normalization were 3.0, -0.4, and 9.5° in the top panel, corresponding to -0.006, 0.001, and -0.017 in the bottom panel, for MSB, BTB, and SRG, respectively.

The lower panel shows the same data plotted in terms of the natural logarithm of HSR at fixation. lnHSR is approximately equal to the magnification of the image in the left eye relative to the right eye; for instance, a lnHSR value of 0.04 corresponds to an image that is 4% larger horizontally in the left eye. The solid horizontal line in the lower panel shows the lnHSR values if no compensation occurred and the dashed diagonal line shows the predicted values for complete compensation. Biases in each observer's settings were again removed: the data were translated vertically until lnHSR was 0 at version = 0°.

These data show that observers are in fact able to set surfaces to objective gaze normal when eye position and VSR cues are consistent with one another and non-stereoscopic cues are rendered uninformative. Thus, observers can set a surface to objective gaze normal based on stereoscopic cues alone.

Observers reported that the surfaces appeared planar which implies that slant was estimated reasonably accurately at non-fixated parts of the surface.

4. Experiment 2: VSR versus eye position

We next asked whether slant estimation by HSR and eye position or by HSR and VSR was the primary determinant of observers' performance in the natural-viewing situation of Experiment 1. To do so, we manipulated eye position and retinal-image information independently.

The retinal images generated by a surface at one azimuth were presented at a variety of eye positions (versions). The predicted slant settings are depicted in the upper left panel of Fig. 11. The solid gray lines are the predictions for HSR and VSR. If settings were based on HSR and VSR, then the observed lnHSR values would vary with the azimuth specified by VSR; this is manifest in the separation of the three lines. Moreover, if settings were based on HSR and VSR, the observed lnHSR values would not vary with eye position; this is manifest in the zero slopes of the prediction lines. The dashed gray line is the prediction for estimation from HSR and eye position. If settings were based on this method, then the observed lnHSR values would not vary with the azimuth specified by VSR (i.e. no separation between the lines), but would vary with version (i.e. non-zero slope).

4.1. Methods

The stimuli were the same as those of Experiment 1 except that the azimuths specified by eye position and VSR were varied independently. All nine possible combinations of versions of −15, 0, and 15° and VSR azimuths of −15, 0, and 15° were presented.

4.2. Results

The remaining three panels of Fig. 11 show the results, a panel for each observer. Biases in each observer's settings were removed by translating the data vertically until lnHSR was 0 for the data point at which version = 0 and VSR azimuth = 0. The data lie close to the horizontal lines that represent the predictions of slant estimation by HSR and VSR. Thus, the data suggest that the primary determinant of perceived slant was the retinal images. However, the data have a small downward slope which implies that there was a small, but consistent, effect of changes in eye position.

The relative influence of slant estimation by HSR and VSR as compared with HSR and eye position can be assessed in another way. Consider estimation by HSR and VSR. According to Eq. (3), as the azimuth specified by VSR is varied the value of lnHSR associated with apparent gaze normal will also vary so as to maintain lnHSR = lnVSR. The amount by which lnHSR actually varies, relative to the amount by which

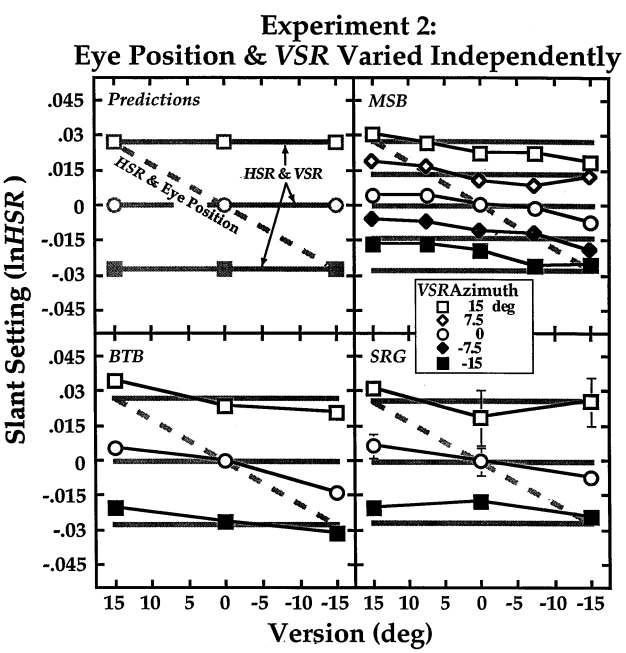

Fig. 11. Predictions and results for Experiment 2. In this experiment, azimuth specified by eye position and azimuth specified by VSR were independently manipulated. The average values of lnHSR for each observer's slant settings are plotted as a function of the eyes' version. The upper left panel shows the predictions: the dashed gray line represents the predictions for slant estimation from HSR and eye position and the solid gray lines represent the predictions for slant estimation from HSR and VSR. The other three panels plot separately the data from the three observers. The symbols represent data for different azimuths specified by VSR: the open squares are for 15°, open diamonds for 7.5, circles for 0, filled diamonds for −7.5, and filled squares for −15°. Error bars correspond to ±1 standard deviation. The data for each observer have again been normalized to 0°. The values subtracted for this normalization were −0.006, 0.001, and −0.017 for MSB, BTB, and SRG, respectively.

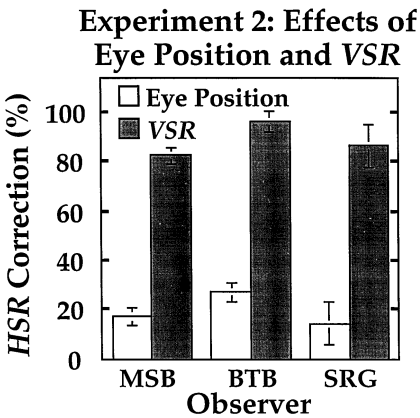

Fig. 12. Eye position and VSR effects in Experiment 2. The percentage change in HSR relative to that needed to compensate completely for changes in azimuth are plotted separately for the three observers. Filled bars represent the percent correction due to changes in VSR and the unfilled bars represent the percent correction due to changes in eye position. The percent HSR Correction values were obtained by fitting a linear model to the data. r^2 values for this fit were 0.93, 0.98, and 0.87 for MSB, BTB, and SRG, respectively. The effects of VSR and eye position were essentially additive. Error bars represent 95% confidence intervals.

lnVSR varies, is therefore a measure of the extent to which the system uses estimation by HSR and VSR to compensate for eccentric gaze. Likewise, the effect of changes in version can be expressed as the amount by which lnHSR varies, relative to the variation expected for accurate use of HSR and eye position (Rogers and Bradshaw, 1993). Fig. 12 shows the percent compensation ('HSR Correction') for changes in azimuth as specified by eye position and VSR, respectively. The unfilled bars represent the effect of eye position and the filled bars the effect of VSR. The percent values were obtained by linear regression on each observer's raw data using coefficients for the effects of eye position, VSR, and individual bias. Error bars represent 95% confidence intervals.

Across observers, the effect of VSR is nearly five times larger than the effect of eye position. For observers MSB and SRG, the combined effects give approximately 100% of the expected compensation. BTB overcompensates for eccentric gaze, presumably because one or both of the slant estimates are inaccurate, or because their weights do not sum to 1.

5. Experiment 3: VSR = 1

The results of Experiment 2 suggest that slant estimation from HSR and VSR is a more significant determinant of perceived slant than estimation from HSR and eye position. The vertical disparities in Experiment 2 were small; the maximum disparity, for instance, was 30 min arc (e.g. at the top left of the stimulus when azimuth specified by VSR was 15°) and this occurred at a retinal eccentricity of 17° where such small disparities might be difficult to measure precisely. Thus, the predominance of slant estimation by HSR and VSR in Experiment 2 is somewhat surprising. We sought to confirm the main finding by reducing all vertical disparities to 0. VSR was 1 at all points in the display (this corresponds in normal viewing to a distant stimulus). If slant judgments for our viewing conditions are indeed based primarily on HSR and VSR, then observers should adjust slant until HSR = VSR. With VSR set everywhere to 1, observers should adjust slant until HSR also equals 1 (lnHSR = 0), as indicated by the solid gray line in Fig. 13. If, on the other hand, slant judgments are based primarily on HSR and eye position, then HSR should vary with the eyes' version as indicated by the dashed gray line.

5.1. Methods

Experiment 3 was identical to Experiment 2 except that all vertical disparities were set to 0 by replacing the image-plane y-coordinate of each dot with that dot's y-coordinate averaged across both eyes' images. Two observers participated. A few measurements were also made with vertical disparity zeroed in Fick coordinates. Azimuths specified by VSR and eye position included all combinations of -15, 0, and 15°, respectively, before vertical disparities were set to 0.

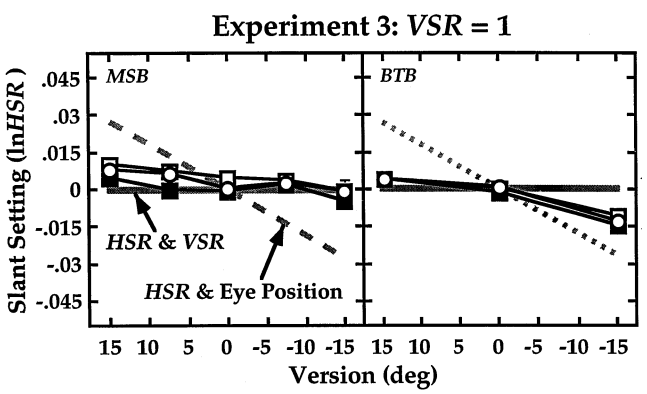

Fig. 13. Predictions and results for Experiment 3. In this experiment, vertical disparities were 0, so VSR was 1 throughout the stimulus. The average values of lnHSR for each observer's slant settings are plotted as a function of the eyes' version. The two panels show data separately for the two observers. The prediction for slant estimation from HSR and eye position is represented by the dashed gray line in each panel and the prediction for estimation from HSR and VSR by the solid gray line. The symbols represent data for different azimuths specified by the retinal images prior to setting vertical disparities to 0: the open squares are for 15°, circles for 0, and filled squares for -15°. Error bars correspond to ± 1 standard deviation. The data have been normalized by -0.005 and -0.002 for MSB and BTB, respectively.

5.2. Results

Fig. 13 plots the average slant settings as a function of the eyes' version. Biases in each observer's settings were removed by translating the data vertically until lnHSR was 0 for the data point at which version = 0 and VSR azimuth = 0. The data are very close to the predictions of slant estimation by HSR and VSR; specifically, the slope of the lnHSR values was close to 0 in all cases. As in Experiment 2, there was a small effect of eye position. Setting vertical disparities to 0 in Fick co-ordinates yielded precisely the same effect as when they were set to 0 in image plane co-ordinates (data not shown).

These data confirm that the primary determinant of slant judgments for the conditions of Experiments 1 and 2 is slant estimation by HSR and VSR rather than estimation by HSR and eye position. The effect of eye position, as determined by linear regression on the raw data, was $16 \pm 3\%$ (0.95 confidence interval) of the full-constancy prediction for MSB, and $31 \pm 4\%$ for BTB.

Both observers reported that surfaces in this experiment appeared convex, similar to a vertically oriented hyperbolic cylinder. This is expected from slant estimation by HSR and VSR (Eq. (3)). Consider a gaze-normal surface in forward gaze ($\gamma = 0$) before VSR was altered. A small patch to the right of fixation would give rise to a VSR less than 1 and to an HSR/VSR ratio less than 1. Thus, setting VSR to 1 decreases the HSR/VSR ratio, which, according to Eq. (3), should increase the perceived slant. As a consequence, if the surface appeared planar before VSR was set to 1, it should appear convex afterward.

6. Experiment 4: vertical lines

Experiments 1–3 revealed little effect of eye position on perceived slant; instead, the visual system seemed to rely on information contained in the retinal images. In terms of underlying mechanisms, there are two ways to interpret this finding.

First, as implied by our model, the visual system might rely on the more reliable of the available signals. Specifically, with the stimuli and viewing conditions of Experiments 1–3, VSR may have been a more reliable indicant of the HSR correction needed than sensed eye position was. If this hypothesis is correct, then altering the measurability of VSR should reduce the visual system's reliance on VSR and increase its reliance on eye position.

Second, the visual system might always rely more on slant estimation by HSR and VSR than on slant estimation by HSR and eye position. If this is correct, then changing the measurability of VSR should not change the system's reliance on sensed eye position. Herzau and Ogle (1937), and Amigo (1967), presented evidence against this hypothesis. Their observers positioned a set of smooth vertical rods until they appeared to lie in a gaze-normal plane. Vertical disparities could not be measured because these stimuli had no vertically separated features. Nonetheless, their observers compensated reasonably well for changes in gaze eccentricity. In this case, they must have used sensed eye position to correct HSR. These experiments can be criticized on the grounds that the stimuli provided monocular cues that could have aided the gaze-normal settings. Specifically, the rods had the same diameters, so an observer could perform the task by adjusting the distances to the rods until they all appeared to subtend the same visual angle at the retina[4].

In order to determine whether sensed eye position is used to correct HSR, we used the technique of Herzau and Ogle (1937), and Amigo (1967), to render vertical disparities unmeasurable. Specifically, we replaced the random-dot stimulus of Experiment 1–3 with a series of vertical lines. Because the lines contained no vertically separated features, vertical disparities (and VSRs) could not be measured. We eliminated the monocular cues that were present in Herzau and Ogle's and Amigo's experiments; the method for eliminating such cues is described below.

6.1. Methods

The stimulus was a set of 12 vertical lines on a virtual plane 40 cm from the cyclopean eye. The set of lines subtended $25 \times \sim 14$ deg. The tops and bottoms of the lines were clipped at different heights by apertures close to the eyes and, consequently, VSR and $\partial \mathrm{VSR}/\partial\gamma$ were not measurable. The lines were anti-aliased in a fashion similar to the dots in Experiments 1–3. The azimuth of the stimulus was varied by rotating the haploscope arms; azimuths of -12.5, -6.25, 0, 6.25, and 12.5° were presented. Observers were instructed to maintain fixation on a central marker while inspecting the stimulus. As before, they used key presses to rotate the stimulus plane until it appeared gaze normal.

The vertical lines were always the same width at the CRT, so their widths in the retinal images did not provide a reliable cue to slant. The horizontal angular subtense of the display at the cyclopean eye was constant, and the spacing of the lines was randomized. The lines were back-projected onto the surface (Banks and Backus, 1998)[5] and hence did not provide a cue to

[4] Ogle (1950) represents such data in terms of H, a term related to curvature, and R_0, a term related to skew. Observers could have used the monocular cue described above to adjust R_0 to the appropriate value at different gaze eccentricities.

[5] The lines were back-projected from the cyclopean eye onto the virtual plane *after* rotation of the plane. With this technique, there is no useful slant information in the monocular images.

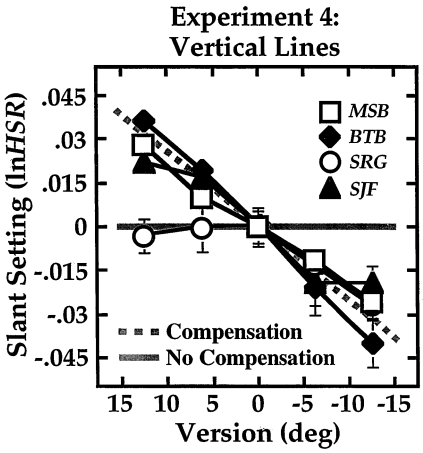

Fig. 14. Predictions and results for Experiment 4. In this experiment, the stimuli were vertical lines, so they contained no VSR signal. The average values of lnHSR for each observer's slant settings are plotted as a function of the eyes' version. The prediction for estimation from HSR and eye position (for interocular distance = 6.0 cm) is represented by the dashed gray line. If no compensation for changes in stimulus azimuth occurred, the data would lie on the horizontal solid gray line. Error bars correspond to ± 1 standard deviation. The data for the four observers are represented by the different symbols. The data have been normalized by 0.002, 0.004, -0.012, and -0.014 for MSB, BTB, SRG, and SJF, respectively.

slant. Thus, there were no reliable monocular cues to slant.

Four observers participated; SRG and SJF were naive to the hypotheses.

6.2. Results

The results are shown in Fig. 14 which plots lnHSR at the slant setting as a function of the eyes' version. If observers used slant estimation by HSR and eye position (and thereby took the eyes' version into account), the data should lie on the dashed diagonal line. If, on the other hand, they did not take the eyes' version into account, the data should lie on the solid horizontal line.

The data for the four observers are represented by the various symbols. Biases in each observer's settings were removed by translating the data vertically until lnHSR was 0 at version = 0 deg. The effects of varying eye position were 78% (0.95 confidence interval: $\pm 6\%$), 118% (± 9), 37% (± 18), and 74% (± 13) of those required for complete constancy for MSB, BTB, SRG, and SJF, respectively.

The data are quite consistent with slant estimation by HSR and eye position except that SRG did not compensate for eye position in leftward gaze. (We do not have an explanation for SRG's undercompensation; it appeared again in Experiment 5.) The results show that extra-retinal, eye-position signals are used to compensate for changes in azimuth when vertical disparities are unmeasurable. Thus, human observers rely heavily on retinal-image information (slant estimation by HSR and VSR) when vertical disparities are measurable, but use sensed eye-position signals (slant estimation by HSR and eye position) when they are made unmeasurable.

7. Experiment 5: height manipulation

Experiments 1–4 revealed little effect of actual eye position on perceived slant unless vertical disparities are rendered unmeasurable. There are many other conditions that affect the magnitude and measurability of vertical disparities, so it is of interest to learn more about the conditions that favor use of vertical disparities as opposed to extra-retinal, eye-position signals.

In Experiment 5, we varied the measurability of VSR by manipulating the height of the surface patch. This manipulation does not affect VSR at a given stimulus location, but it does affect the area over which VSR can be measured and the magnitude of the largest vertical disparities in the display. Either of these factors might affect the visual system's confidence in $\hat{V}SR$. However, this manipulation should not affect the extra-retinal signals from sensed eye position ($\hat{\mu}$ and $\hat{\gamma}$) because these signals should not depend on image size. We expect, therefore, that as display height decreases, the visual system will give relatively more weight to the estimate from HSR and eye position. When display height is near zero, VSR is impossible to calculate, so there should be no effect of the azimuth specified by VSR.

7.1. Methods

Planar surface patches were presented again at a viewing distance of 57.3 cm, as specified by eye position and by the retinal images. The width of the simulated patch varied randomly from 30–34°; this ensured that image width, which is maximum when the patch is gaze normal, was not a reliable slant cue. Four stimulus heights were used: 30, 6.5, 1.3, and 0° (0° had an actual height of one anti-aliased pixel). The displays for those heights contained 400, 100, 70, and 70 dots, respectively. The eyes' version and the azimuth specified by VSR were manipulated independently and took on values of -15, 0, or 15°. Observers made six settings at each combination of height, VSR-specified azimuth, and version. Observers MSB, BTB, SRG, and RVE participated.

Because the number of dots in the display co-varied with the height of the display, a control experiment tested whether dot number or height was the primary determinant of slant settings. Stimulus height was 6.5° and 70 or 400 dots were presented. Observers BTB, SRG, and RVE participated.

7.2. Predictions and results

Fig. 15 displays the predictions (and results) for observer MSB. As before, the horizontal gray lines

represent predicted lnHSR values when slant judgments are based entirely on HSR and VSR; the dashed diagonal line represents predicted lnHSR values when slant judgments are based entirely on HSR and eye position. Biases were removed by translating the data vertically. The slant settings for this observer were very consistent with the predictions of slant estimation by HSR and VSR when the stimulus height was 30° and were very consistent with the predictions of estimation by HSR and eye position when the height was 0 and 1.3°.

Fig. 16 shows the effects of eye position and VSR as a percentage of the compensation required for a 30° change in azimuth. Percent HSR correction (as in Fig. 12) is plotted as a function of stimulus height. When height was 30°, slant settings were quite consistent with slant estimation by HSR and VSR, which replicates the results of Experiment 2. As height was decreased, however, the settings of all four observers departed more and more from those predicted by HSR and VSR and became increasingly consistent with those predicted by HSR and eye position. The effect is simplest in observer MSB: when height was 30°, his settings were very consistent with slant estimation by HSR and VSR; when height was 0°, his settings were very consistent with estimation by HSR and eye position. Observer SRG exhibited a similar effect, but she under-compensated for changes in version as stimulus height was reduced. Observers BTB and RVE also exhibited the primary effect, but they over-compensated for changes in version when height was 0°; interestingly, BTB over-compensated much more in rightward than leftward gaze, and the amount of over-compensation was larger than in Experiment 4[6,7]. Averaging the data from all

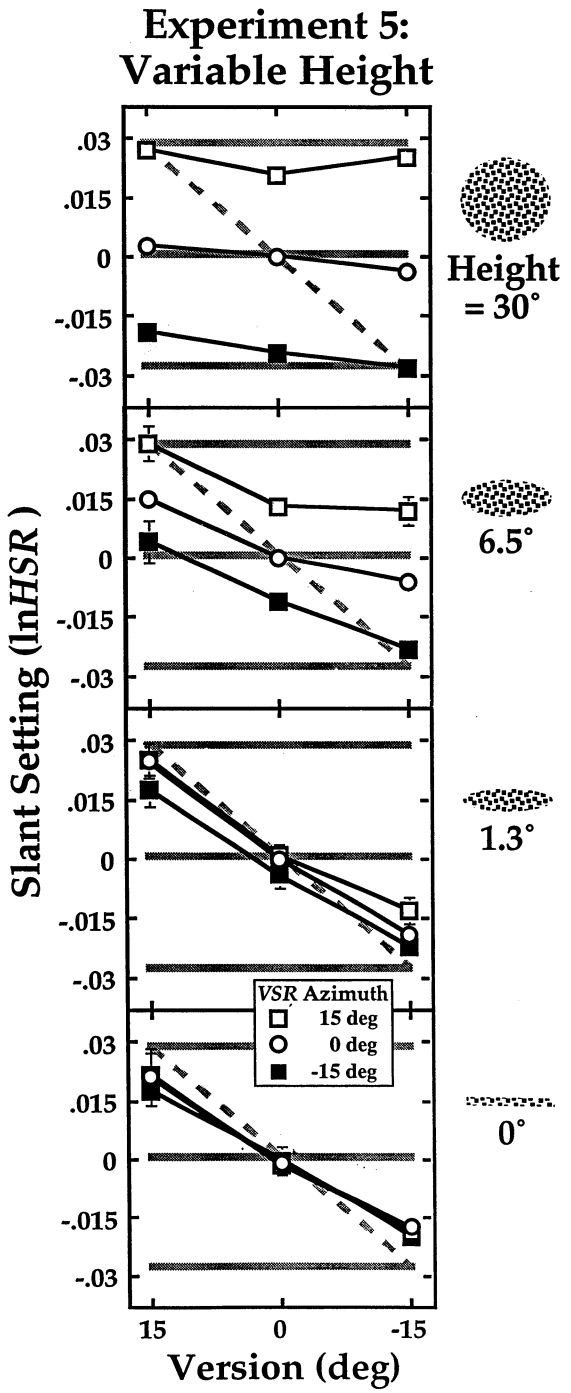

Fig. 15. Predictions and results for observer MSB in Experiment 5. The stimuli were similar to those in Experiment 2 (randomly positioned dots defining a plane), but stimulus height was varied. Average values of lnHSR for the slant settings of this observer are plotted as a function of the eyes' version. The dashed gray line represents the predictions for slant estimation from HSR and eye position and the solid gray lines represent the predictions for slant estimation from HSR and VSR. The icons to the right represent the stimuli. From top to bottom, the panels show data corresponding to stimulus heights of 30, 6.5, 1.3, and 0°. The symbols represent data for different azimuths specified by retinal images: the open squares are for 15°, circles for 0, and filled squares for −15°. Error bars correspond to ±1 standard deviation. The data for each stimulus height have been normalized; the values subtracted were 0.004, −0.001, −0.004, and −0.005 for heights of 30, 6.5, 1.3, and 0°, respectively.

[6] That some observers make large, systematic errors when estimting slant from HSR and eye position suggests that this method is not normally a major determinant of perceived slant (van Ee and Erkelens, 1996). Note also that if an estimate is biased, as here, its weight in a cue-conflict condition is not given accurately by a 'percent compensation' statistic (such as percent HSR correction in Fig. 16); cf Landy et al. (1995), Rogers and Bradshaw (1995). A reasonable way to determine the weight of a biased estimator is to divide the effect (perturbation) obtained in the cue-conflict condition by the effect obtained when only the estimate of interest is computable (i.e. when its weight is 1 by definintion). Using this procedure, weights can be derived for the HSR and eye position estimate of slant in Experiment 5 by normalization relative to data from Experiment 4 or the 0° height condition of Experiment 5. These weights are smaller for BTB and RVE , and larger for MSB and SRG, than the percent compensation data (open squares) shown in Fig. 16.

[7] BTB and RVE normally wear spectacles. Both are myopic, so their spectacles minify. Thus, they normally fixate by making an eye turn that is smaller than the head-centric azimeuth of the target. For example, BTB requires a 15° eye turn to foveate a target at 18°. This relationship between target azimuth and required eye turns might affect estimates that use eye position. BTB and RVE wore contact lenses during the experiment, so fixation at a given azimuth required a larger than normal eye turn, which could yield a larger effect of version on perceived slant than expected.

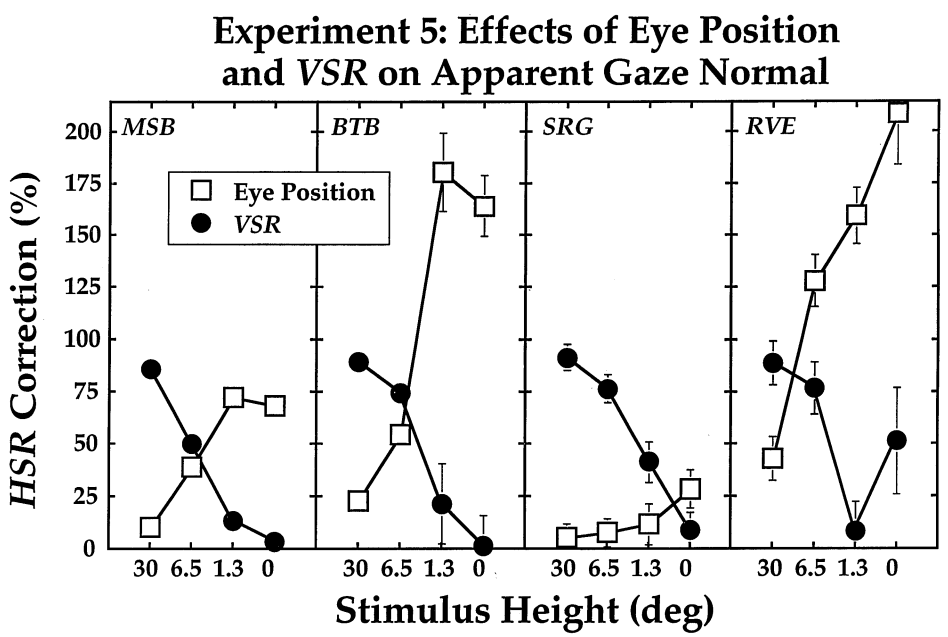

Fig. 16. Eye position and VSR effects in Experiment 5. The percentage change in HSR relative to that needed to compensate completely for changes in azimuth are plotted separately for the four observers; they are plotted as a function of stimulus height. Filled circles represent the percent correction due to changes in VSR and the unfilled squares represent the percent correction due to changes in eye position. The percent HSR Correction values were obtained by fitting a linear model to the data (see text for details). r^2 values for linear fits from the tallest to shortest display were 0.98, 0.92, 0.96, and 0.95 for MSB, 0.98, 0.96, 0.88, and 0.91 for BTB, 0.94, 0.91, 0.60, and 0.47 for SRG, and 0.87, 0.92, 0.91, and 0.85 for RVE. The effects of VSR and eye position were essentially additive. Error bars represent 95% confidence intervals.

three observers in Experiment 2 and the 30° height data from all four observers in Experiment 5, the effect of VSR was $88 \pm 2\%$ (standard error) of that predicted by Eq. (3).

In the control experiment, we asked whether the transition from VSR-based to eye-position-based estimation was determined primarily by stimulus area or by the number of visible dots. Stimulus height was fixed at 6.9°, and 70 or 400 dots were visible. The experiment was otherwise similar to Experiment 5. There was no discernible effect of dot number; thus, with the dot numbers we used, stimulus area (or height), and not dot number (or density), was the controlling variable.

The data from Experiment 5 imply that slant estimation by HSR and VSR and by HSR and eye position are both used in determining the slant of a stereoscopically defined surface. Furthermore, human observers seem to rely most on the VSR-based method when the stimulus is large and most on the sensed-eye-position method when it is small. A similar conclusion concerning perceived curvature has been drawn by Rogers and Bradshaw (1995).

8. Discussion

8.1. Is slant initially represented in oculocentric or headcentric coordinates?

In most models of stereoscopic slant estimation (e.g. Gårding et al., 1995; Koenderink and van Doorn, 1976), slant is estimated relative to the line of sight (Gillam et al., 1988); that is, slant is estimated in oculocentric coordinates. Our model (Fig. 7) shares this feature. Under this assumption, the observer must make a number of co-ordinate transformations to obtain slant in bodycentric co-ordinates, as would be useful for motor behaviors such as reaching and grasping.

Gillam and Lawergren (1983), and more recently Erkelens and van Ee (1998), proposed that slant is estimated first relative to the head. This proposal is appealing because headcentric disparity patterns are independent of eye position and, therefore, no transformation is required from oculocentric to headcentric coordinates after the surface slant has been estimated. Nonetheless, it is more likely that slant is represented first oculocentrically for two reasons.

First, the oculocentric task of making a stereoscopic surface perpendicular to the line of sight (the gaze-normal task) is subjectively easier than the headcentric task of making it parallel to the forehead. Estimation first in headcentric co-ordinates requires that the slant estimate be transformed into oculocentric co-ordinates for the gaze-normal task. This would make the gaze-normal task harder, not easier, than the parallel-to-forehead task, because the gaze-normal task would require an additional transformation. In terms of signals, $\hat{\gamma}$ would have to be used twice in the gaze-normal task: first to

determine the headcentric directions of the points in space that gave rise to the disparity pattern (Erkelens and van Ee, 1998), and then again to determine where on the head-centrically defined surface one is looking. This double usage increases susceptibility to noise in $\hat{\gamma}$. If slant is calculated first oculocentrically, then $\hat{\gamma}$ is not needed for the gaze-normal task, but is needed for the headcentric task; this may explain why the gaze-normal task is subjectively easier.

Second, perspective cues contain slant information in oculocentric co-ordinates only, so the integration of perspective and stereoscopic slant estimates would be computationally simpler in oculocentric co-ordinates. The same would be true for a slant estimate based on retinal-image motion cues (Braunstein, 1968; Koenderink and van Doorn, 1975; Longuet-Higgins and Prazdny, 1980).

The gaze-normal task is well-suited for oculocentric co-ordinates. There may be stereoscopic tasks in which performance is more accurate in head- than in oculo-centric co-ordinates, but until such a task is identified, we favor the more conventional assumption that slant estimation via stereopsis is done oculocentrically.

8.2. Additivity of VSR and eye position effects

In the cue-conflict experiments (Experiments 2 and 5), the effects of azimuth specified by eye position and VSR were roughly additive. A linear fit accounted for most of the variance in the data. The good fit of the linear model suggests that the slant estimates are independent to the extent that the estimate from HSR and VSR does not change with eye position, and the estimate from HSR and eye position does not change with VSR. It also suggests that perceived slant can be modeled as a weighted average of separate slant estimates as in Fig. 7.

Our experiments involved the presentation of stimuli with properties that never arise in natural viewing. For example, some of the conditions of Experiments 2 and 5 involved stimuli for which VSR and sensed eye position specified completely different azimuths. In such situations, observers might have access to two separate percepts, one based on VSR and the other on eye position. If there were two percepts, one or the other would determine the response on a given trial. Alternatively, the visual system might produce one slant estimate based on a weighted combination of the estimates arising from HSR and VSR and from HSR and eye position (as suggested by the model in Fig. 7). There are two pieces of evidence that imply that the latter is a better description. First, the appearance of the stimuli was similar whether VSR and eye position conflicted or agreed; in both cases, the stimuli appeared planar and the slant was well-specified. Second, the variability of slant settings was not markedly higher in the conflict conditions. The standard deviations were only slightly higher when VSR and eye position specified opposite azimuths (e.g. -15 and 15°) than when they specified the same azimuths: the average ratio of standard deviations (conflict/natural) was 1.6 in Experiment 2 and the 6.5 and 30° conditions of Experiment 5. Thus, the conflict between slant estimates causes only a small increase in the variability of slant settings which is consistent with the idea that the observers' settings are based on one slant estimate, determined possibly in the fashion suggested by Fig. 7.

Curiously, several observers showed large systematic biases in perceived slant (SRG in Experiments 1, 2, 4, and 5; SJF in Experiment 4; RVE in Experiment 5, not shown; see captions to Figs. 10, 11 and 14). The cause is not clear. Biases in signal estimates or errors in their use could have this effect. For example, horizontal meridional aniseikonia of 1.2–1.7% (image effectively larger in the right eye) would account for the bias in SRG's settings (see Howard and Rogers, 1995).

8.3. Weighted averaging of simultaneous estimates versus sequential stages

Ogle (1940, 1950) believed that VSR and eye position stimulated two separate mechanisms for stereoscopic slant constancy in eccentric gaze. First, a 'psychic' response, triggered by vertical disparity, alters the stereoscopic frame of reference; he believed that the induced effect is a manifestation of this response. Second, a 'physiologic' mechanism, triggered by rotation of the eyes into eccentric gaze, causes an internal, overall magnification of one eye's image relative to the other, so that 'a change in the relative functional sizes of the ocular images of the two eyes occurs in the vertical meridian when the eyes are turned in asymmetric convergence and that in general this change is of an amount which offsets the difference in the distance of the observed object from the two eyes' (Ogle, 1940).

Ogle did not state how the mechanisms functioned together, but given his description of the physiologic mechanism, there is only one sensible interpretation: the images are first adjusted in overall size according to sensed eye position and then the vertical disparities that remain are used to interpret the residual horizontal disparities. Bishop (1994, 1996), made this hypothesis explicit: he proposed that size scaling based on eye position occurs first and then correction based on VSR occurs. Bishop's hypothesis is unattractive because it fails to explain why the perceived sizes of retinal images

differ when one holds steady fixation on an eccentric object (Ogle, 1939b; Schor et al., 1994)[8].

8.4. Eccentricity and vertical magnification have similar effects on vertical disparity

Vertical disparity is frequently manipulated by placing a vertical magnifier before one eye while viewing a real object (Ogle, 1950; Gillam et al., 1988). It was manipulated in our experiments by presenting synthetic images of surfaces at different simulated azimuths. Clearly, vertical disparity at fixation can be altered by either means, but do the two manipulations have the same effect on the pattern of vertical disparities across the stimulus? We examine here the disparity patterns created by eccentric gaze and by unilateral vertical magnification. Vertical disparity is zero along the horizontal meridian, so it is more appropriate to look at VSR. Fig. 17 shows lnVSR as a function of retinal eccentricity for three gaze-normal planes: azimuths (γ) = 0 and 15°, and azimuth = 0° but seen through a 2.7% vertical magnifier before the left eye. The patterns of VSR across the latter stimuli are nearly identical for retinal eccentricities out to $\pm 15°$; with greater eccentricity, the patterns diverge. Thus, eccentric viewing and vertical magnification have nearly identical effects for our stimuli (radius $\leq 20°$). Accordingly, it is appropriate to compare our findings to those obtained in the literature on the induced effect.

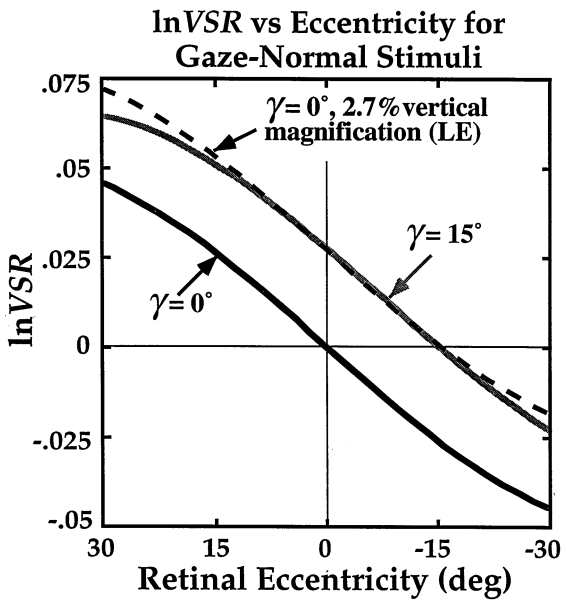

Fig. 17. VSR as a function of retinal eccentricity with unilateral vertical magnification or eccentric gaze. lnVSR is plotted as a function of horizontal retinal eccentricity for three planar surfaces: a gaze-normal surface at an azimuth of 0° (solid black curve), the same surface viewed with a 2.7% vertical magnifier in front of the left eye (dashed black curve), and a gaze-normal surface at an azimuth of 15° (solid gray curve). The viewing distance is 57.3 cm. For stimuli smaller than 20° in radius, vertical magnification and eccentric gaze have very similar effects on VSR across the image.

[8] Some researchers found evidence for eye-position-based magnification. In eccentric gaze, dichoptic images that are actually the same size can appear to be of different sizes (Ames et al., 1932; Ogle, 1939a). However, this effect is visible only when observers are allowed to move their eyes (Ogle, 1939a). We now know that saccadic eye movements in eccentric gaze are unequal, as is required for accurate fixation (Schor et al., 1994). It seems likely that when Ogle's subjects were allowed to make saccades across the target, the resulting fixation disparity caused the apparent size change. Curiously, Ogle himself noted that a coin viewed in eccentric gaze appears larger in the closer eye. This demonstration would fail if eye position were used to correct image sizes.

8.5. Induced effect revisited

In the induced effect, a vertical magnifier placed before one eye causes a frontoparallel surface to appear rotated about a vertical axis. This phenomenon was first reported by Lippincott (1889) and Green (1889), but Ogle (1938, 1939a,b, 1940, 1950), made the first systematic measurements. To restore the appearance of frontoparallelism, the surface must be rotated away from the magnified eye; the direction of this rotation is predicted by Eq. (3), that is, by slant estimation using HSR and VSR.

Fig. 18 shows induced-effect data from Ogle (1938). The left panel shows the slant of the stimulus plane when it appeared gaze normal as a function of the vertical magnification of the left or right eye's image. The right panel shows the same data when lnHSR in the retinal images is plotted as a function of lnVSR. The solid lines represent predicted slant settings for estimation by HSR and VSR. Notice that the induced effect follows predictions up to roughly 4% magnification ($-0.04 \leq \ln\mathrm{VSR} \leq 0.04$), but deviates from the predictions at higher magnifications; frequently, plateaux are observed at the higher magnifications. The agreement between observed and predicted settings at low magnifications varies from one study to another; in some (Ogle, 1938), the agreement is excellent, but in others (Ogle, 1939a, 1940; Gillam et al., 1988), the observed settings fall systematically short of prediction.

The existence of the induced effect is strong evidence that vertical disparities are used to interpret horizontal disparities as in the method of slant estimation from HSR and VSR (Eq. (3)). However, the induced-effect plateaux have resisted explanation. With magnification of one eye's image, the natural relationships among HSR, VSR, sensed eye position, and perspective are altered. In Ogle's (1938) induced-effect experiment, the introduction of vertical magnification affected VSR only. Consequently, slant estimation by HSR and VSR indicated that an objectively gaze-normal surface was rotated, but estimation by HSR and eye position and estimation by perspective indicated that the surface was

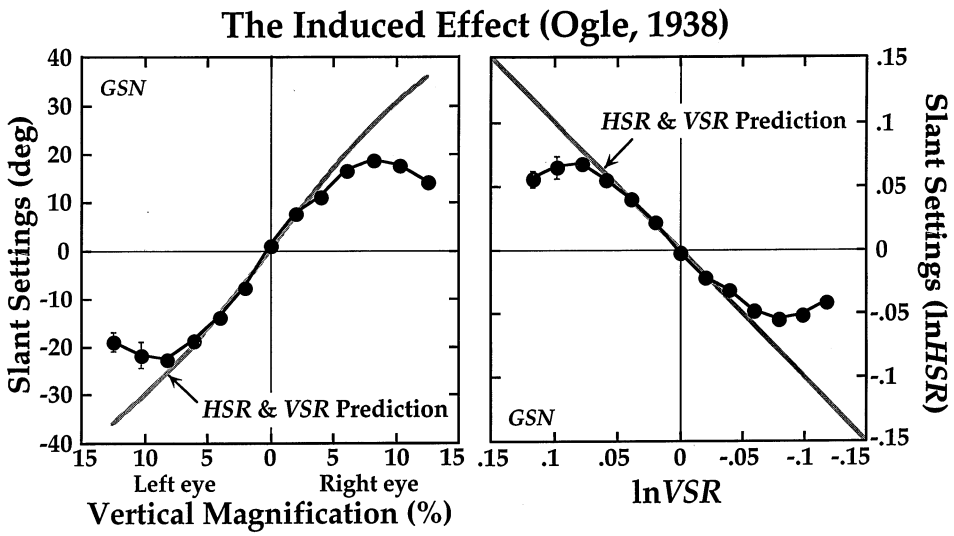

Fig. 18. The induced effect as reported by Ogle (1938). The panel on the left plots the observer's slant settings as a function of the percent vertical magnification applied to the left or right eye. The panel on the right plots the same data, but the abscissa is lnVSR, and the ordinate is lnHSR (when slant was negative, lnHSR was positive). Error bars indicate ± 1 standard deviation. The solid lines show the slant setting predicted by slant estimation from HSR and VSR (Eq. (3)). Adapted from Ogle (1938).

not rotated. Banks and Backus (1998) argued that the plateaux in the induced effect (and their absence for a horizontal magnifier) are due to conflicts among the various means of estimating slant. Here we examine the plateaux in greater detail and show that they can be explained in terms of the signals involved.

Let us call the three slant estimates $\hat{S}_{\mathrm{HSR,EP}}$, $\hat{S}_{\mathrm{HSR,VSR}}$, and $\hat{S}_{\mathrm{P}}$. The model presented in Fig. 7 combines the estimates linearly after each estimate is given a weight based on ancillary cues (such as spatial pattern, display height, or the estimated signals). It is a 'modified weak fusion' model in the terminology of Landy et al. (1995). In the induced effect, $\hat{S}_{\mathrm{HSR,EP}}$ and $\hat{S}_{\mathrm{P}}$ are similar to one another, and both are dissimilar from $\hat{S}_{\mathrm{HSR,VSR}}$. A sensible strategy is to give the usual weights to all three estimates when they differ slightly, but to decrease the weight given to the discrepant estimate when it differs greatly from the other two. This is a robust estimation strategy because an estimate that differs significantly from other independent estimates (that agree with one another) is probably the least accurate estimate under normal viewing conditions. It is interesting to note that the induced-effect curve is remarkably similar in shape to the theoretical 'influence curve' of a robust estimator (Fig. 3 in Landy et al. (1995)).

In the experiments presented in this paper, VSR at fixation had a maximum value of 1.027 (when azimuth specified by VSR was 15°). A surface in forward gaze viewed with a 2.7% vertical magnifier in front of the left eye creates the same proximal VSR (Fig. 17). Thus, our stimuli are within the range of magnifications for which the induced effect generally follows the predictions of slant estimation by HSR and VSR. Indeed, we observed a large effect of VSR: the effect was $88 \pm 2\%$ of that predicted by (Eq. (3)) see (Experiment 5 results).

When perspective cues are rendered uninformative, as in Experiment 1 of Banks and Backus (1998), only $\hat{S}_{\mathrm{HSR,EP}}$ and $\hat{S}_{\mathrm{HSR,VSR}}$ are available. When they disagree at high magnifications in the induced effect, there is no third estimate to help determine which estimate is most veridical. Thus, a modified weak fusion model (Landy et al., 1995) predicts no plateaux. Banks and Backus (1998) in fact observed no plateaux, even at vertical magnifications up to 15%, when perspective cues were made uninformative.

The effect of small vertical magnifications in Ogle (1938) (Fig. 18) is 100% of the HSR and VSR prediction, suggesting a weight of 1 for $\hat{S}_{\mathrm{HSR,VSR}}$ and a weight of 0 for $\hat{S}_{\mathrm{HSR,EP}}$ and $\hat{S}_{\mathrm{P}}$. Our data fell short of the HSR and VSR prediction: the average effects of vertical magnification were $88 \pm 2\%$ in the present work and $84 \pm 3\%$ in Banks and Backus (1998). The data of Ogle (1939a, 1940), also fell short of the predictions even at small magnifications (see Figs. 19 and 20). We attribute these shortfalls to non-zero weighting of $\hat{S}_{\mathrm{HSR,EP}}$ and, when perspective is present, to nonzero weighting of $\hat{S}_{\mathrm{P}}$ as well. Thus, in most cases, some weight is probably given to $\hat{S}_{\mathrm{HSR,EP}}$ and $\hat{S}_{\mathrm{P}}$ even at small magnifications. It remains to be determined why Ogle's (1938) experiment essentially eliminated eye position and perspective effects while other experiments did not.

8.6. Eccentric gaze revisited

Ogle (1940) measured induced-effect functions during eccentric gaze or with overall magnification of one eye's image. He pointed out that for every eccentric gaze

position, there is an overall magnification that yields very nearly the same pattern of binocular disparities with the eyes in forward gaze. He had observers view the same pattern of disparities with the eyes forward (overall-magnification condition) or turned to the side

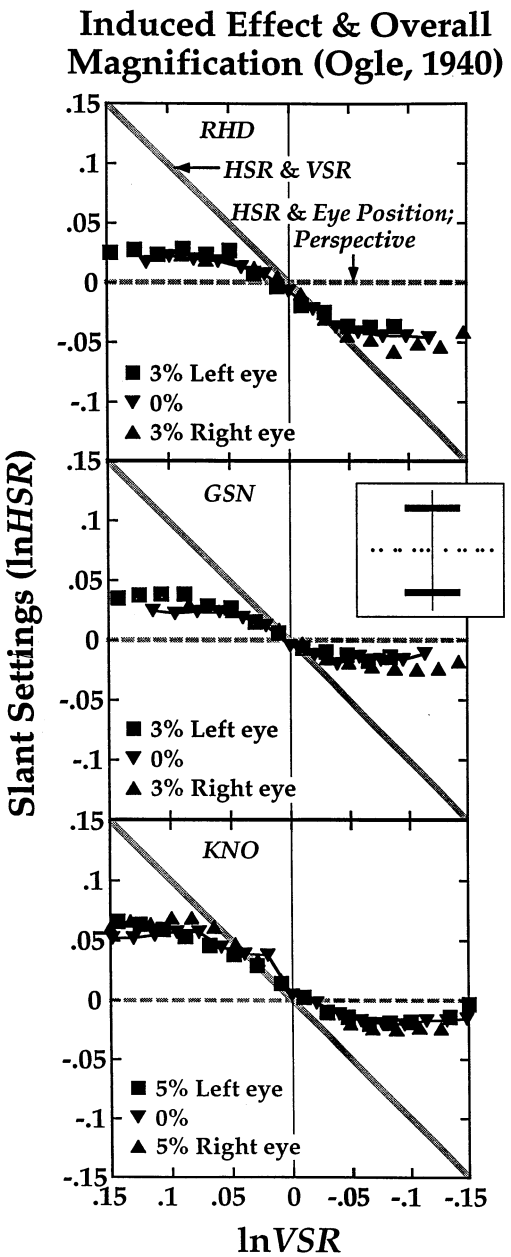

Fig. 19. The effect of overall magnification on the induced effect as reported by Ogle (1940); see text for details. Observers' slant settings in terms of lnHSR are plotted as a function of lnVSR. Each panel shows the data from a different observer. For observers RHD and GSN (upper and middle panels), the lenses produced 3% magnification of the left eye's image (square symbols), 3% magnification of the right eye's image (upright triangles), or 0% magnification (inverted triangles). For observer KNO (lower panel), the lenses produced 0% (inverted triangles) or 5% magnification (squares and upright triangles). The 0% overall magnification data in each panel are connected with a line; the other data are not. Adapted from Ogle (1940).

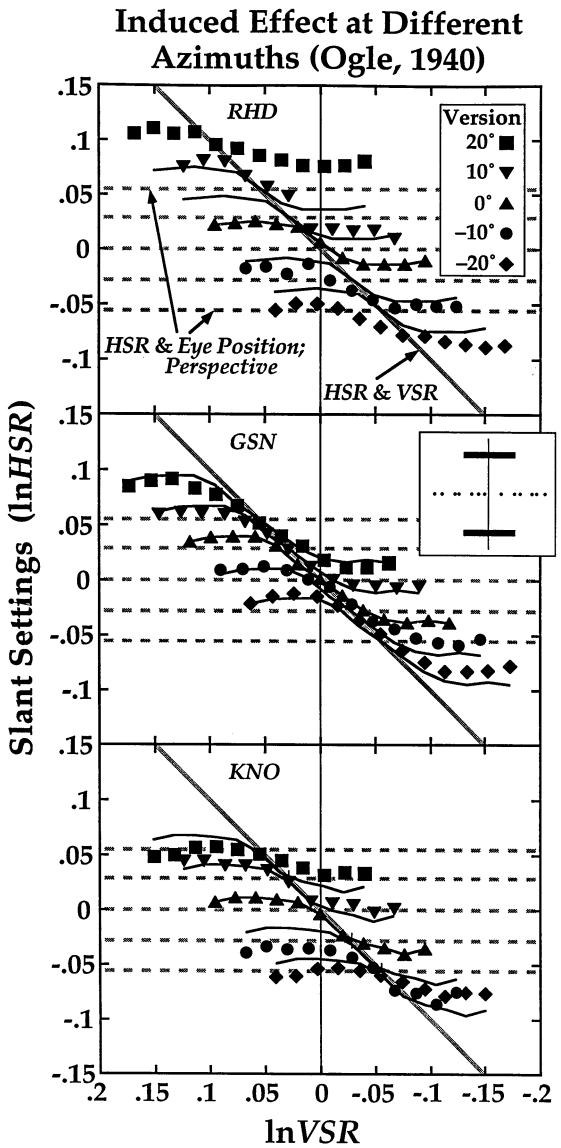

Fig. 20. The effect of eccentric gaze on the induced effect as reported by Ogle (1940); see text. Observers viewed the stimulus at different eccentricities such that the eyes' version was −20° (diamonds), −10 (circles), 0 (upright triangles), 10 (inverted triangles), or 20° (squares). Prediction lines are based on an average interocular distance of 6.5 cm reported by Ogle for his observers. The data from the 0° version condition have been connected by lines and those lines have been translated diagonally according to the changes in lnHSR and lnVSR due to the change in version. Adapted from Ogle (1940).

(eccentric-gaze condition). If slant percepts were determined by the pattern of retinal disparities alone (slant estimation by HSR and VSR), apparent gaze-normal settings should have been identical in the two conditions (although Ogle's writing is not clear on this point). If, however, slant percepts were also affected by the sensed positions of the eyes (slant estimation by HSR and eye position), settings should have differed in the two conditions.

The stimulus was a row of horizontal dots and two small rectangles positioned above and below the dot

row (icons in Figs. 19 and 20). The vertical magnification of one eye's image was varied systematically. Observers rotated the stimulus about a vertical axis until it appeared gaze normal.

In the overall-magnification condition, a lens (magnifying equally in the vertical and horizontal meridia) was placed before one eye and VSR was manipulated by an additional vertical magnifier. Three values of overall magnification were used for each observer. As Ogle expected, induced-effect functions (such as the function in the left panel of Fig. 18) shifted diagonally with changes in overall magnification (see Figs. 5–7 in Ogle (1940)). The shift was up and to the right with increasing magnification of the left eye's image.

It is informative to plot the HSR and VSR values in the retinal images. Fig. 19 plots lnHSR as a function of lnVSR. Each panel shows the data from one of Ogle's three observers.

The three means of slant estimation described earlier make different predictions for these data (see also Banks and Backus, 1998). According to slant estimation by HSR and VSR, HSR should be equal to VSR at the observers' settings; this prediction is represented by the diagonal line in each panel of Fig. 19. According to slant estimation by HSR and eye position, the addition of overall magnification should have no effect on the data when plotted in terms of the proximal HSR because $\hat{S}_{\mathrm{HSR,EP}} = 0$ in forward gaze when $\ln\mathrm{HSR} = 0$; this prediction corresponds with the dashed horizontal line in each panel. The dots and the rectangular inducing figures create a strong perspective cue, so we cannot ignore perspective information in Ogle's (1940) experiment. According to slant estimation by perspective, a surface is perceived as gaze normal whenever the perspective gradient is minimized (Sedgwick, 1986). In Ogle's set-up, this also yields the dashed horizontal line in each panel, the same prediction as for slant estimation by HSR and eye position.

Our replotting of the overall magnification results makes very clear that observers' slant settings were simply those that produced the same HSR value at a given value of VSR. Stated another way, the proximal HSR values associated with a gaze-normal percept were a function of proximal VSR, and were unaffected by overall magnification. The observers' settings at low magnifications are reasonably well predicted by slant estimation from HSR and VSR (the solid diagonal line), but settings at high magnifications are not well-predicted by this means of estimation. As before, according to our conceptualization, the plateaux observed at high vertical magnifications are the result of conflicts between $\hat{S}_{\mathrm{HSR,VSR}}$ on the one hand and $\hat{S}_{\mathrm{HSR,EP}}$ and $\hat{S}_{\mathrm{P}}$ on the other. The conceptualization presented here predicts that the data in this experiment should superimpose and they do.

In the eccentric-gaze condition of Ogle's (1940) experiment, observers viewed the same stimulus and performed the same task as before, but they now turned their eyes to view the stimulus at azimuths of -20 to 20°. In discussing his predictions for this experiment, Ogle focused on horizontal displacements of induced-effect functions (see Figs. 8–10 in Ogle (1940)), but more complete predictions were possible as we will see. The results showed smaller displacements than one would predict from the overall magnification data, so Ogle concluded that he had demonstrated a compensation for overall magnification in eccentric gaze triggered by the eyes' version (Ogle, 1940).

Fig. 20 plots Ogle's eccentric-gaze data in terms of proximal HSR and VSR. Overall magnification and eccentric viewing have nearly the same effect on HSR and VSR (assuming a surface of fixed slant), so the data would be identical in Figs. 19 and 20 if there were no compensation based on sensed eye position. Clearly, the data are not identical, but does this really provide evidence for compensatory changes triggered by version eye movements? We believe it does not for the following reason.

Two of the three means of slant estimation described earlier make different predictions for the eccentric-gaze than for the overall-magnification condition. The prediction for slant estimation by HSR and VSR is again a diagonal line along which $\mathrm{HSR} = \mathrm{VSR}$. However, according to slant estimation by HSR and eye position, changes in the eyes' version should affect the slant settings because for each version, a different HSR value is required to establish a gaze-normal percept (Eq. (2)); this means of slant estimation yields the five dashed horizontal lines, one for each version. Slant estimation by perspective yields the five dashed horizontal lines in each panel, the same predictions as for slant estimation by HSR and eye position.

Because slant settings differed in the two conditions, Ogle (1940), thought he had demonstrated that sensed eye position is used to interpret horizontal disparities. Our plots of Ogle's (1940) data reveal, however, that the differences in slant settings could have been caused by differences in the slants indicated by perspective cues. Stated another way, one cannot determine from Ogle's data whether the differences in perceived slant in the two conditions were a consequence of using perspective information, eye-position signals, or both.

In related work, the ability to compensate for changes in gaze eccentricity was measured when the stimulus was a set of vertical rods (Amigo, 1967; Herzau and Ogle, 1937). Observers adjusted the distance to each rod until the rods appeared to lie in a gaze-normal plane. The rods contained no vertically separated features, so no vertical disparity signal was available. Consequently, the experimenters reasoned that performance in this task provided a measure of the

ability to use sensed eye position to interpret horizontal disparities. If observers did not take changes in the eyes' version into account, settings would have been in the plane tangent to the Vieth-Müller Circle (where HSR = 1). If they compensated completely for version changes, they would have set the rods in the objective gaze-normal plane.

Herzau and Ogle (1937) found essentially complete compensation at all gaze eccentricities (− 24.8–24.8°). Amigo (1967) found partial compensation: the rods were positioned, on average, about halfway between the objective gaze-normal plane and the plane tangent to the Vieth-Müller Circle. The experimenters concluded, therefore, that they had demonstrated the use of sensed eye position to interpret horizontal disparities. In both studies, however, salient perspective cues were again present. The rods were all the same diameter in Herzau and Ogle (1937), so observers could have performed the task by adjusting the distances until rod pairs on opposite sides of the fixation point subtended the same angle in one eye. The rod diameters varied in Amigo (1967), but were the same for pairs at the same eccentricities from the central rod; therefore, observers could have performed this task using the same strategy. As with Ogle (1940), perspective-based slant estimation and eye-position-based estimation make the same predictions, so one cannot determine their respective contributions.

Banks and Backus (1998) argued that the plateaux and the variations in magnitude observed in the induced effect can be understood from an analysis of all the signals involved in performing this task. In particular, they argued that full induced effects without plateaux can be observed if one eliminates conflicting slant information from perspective and eye position. We can illustrate this point with data from two of their three experiments. Fig. 21 plots the data in terms of HSR and VSR at the retinae; the two panels show data from observers MSB and BTB who also participated in all the experiments of the current paper. In their first experiment, Banks and Backus (1998) measured the induced effect with the observers' eyes in forward gaze ($\gamma = 0$) and with perspective conflicts, as in the classic induced effect experiments (Ogle, 1938). The data from that experiment are represented by the filled squares. Notice that induced-effect plateaux are clearly observed under these circumstances. In their third experiment, Banks and Backus measured the induced effect with the observers' eyes in eccentric gaze (γ was equal to the azimuth specified by VSR in the images) and with perspective cues rendered uninformative. In this situation, $\hat{S}_{\mathrm{HSR,VSR}}$ and $\hat{S}_{\mathrm{HSR,EP}}$ are the same and no weight is given to $\hat{S}_{\mathrm{P}}$. The data from that experiment are represented by the open squares. The plateaux are eliminated and full induced effects are observed up to the highest magnifications presented. Thus, cases in which the induced effect plateaus (e.g. Ogle, 1938) can be understood from an analysis of all the signals and conflicts involved.

8.7. Stimulus height and the induced effect

In Experiment 5, we observed that slant settings were determined primarily by slant estimation from HSR and VSR for tall stimuli and by slant estimation from HSR and eye position for short stimuli. This result appears to conflict with some observations by Ogle (1939a), so we re-examine Ogle's observations here.

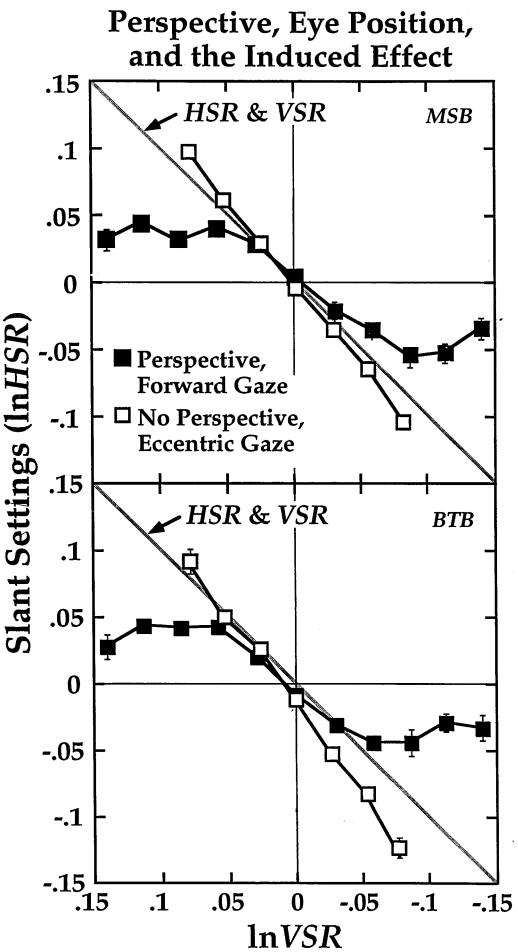

Fig. 21. The effect of perspective and sensed eye position on the induced effect as reported by Banks and Backus (1998). Observers' slant settings in terms of lnHSR are plotted as a function of lnVSR. The panels show the data from two observers separately. The solid diagonal lines represent the predictions for slant estimation from HSR and VSR. The data were collected in two conditions. In one, the eyes' version was 0° (forward gaze) and the stimulus contained clear perspective cues to slant (see Banks and Backus (1998)). The data from this condition are represented by the filled squares. In the other condition, the eyes' version was equal to the azimuth specified by VSR in the stimulus and the stimulus did not contain informative perspective cues. The data from this condition are represented by the unfilled squares. Error bars represent ± 1 standard deviation.

Ogle (1939a) measured induced-effect functions with a stimulus consisting of a horizontal row of dots and two horizontal rectangles positioned above and below the dot row. The vertical separation between the rectangles was varied from 2–23°. Both the width and the height of the rectangles were proportional to their separation. The stimulus was viewed in forward gaze with a vertical magnifier placed before one eye; Ogle found that the resulting induced-effect functions varied little from one separation to another.

In Experiment 5, we found that VSR variations had a marked effect on slant settings when stimulus height was 6.5° or higher and had little effect on settings for shorter stimuli. Thus, we found that the use of VSR depended on stimulus height and Ogle (1939a) did not. To what can we attribute the difference in outcomes?

In Ogle's experiment, $\hat{V}SR$ was necessarily determined from the horizontal rectangles because the horizontal dot row by itself contained no vertically separated features from which to measure VSR. Thus, estimation of VSR was based on widely separated features whose size was proportional to their retinal eccentricity. It is well-known that visual sensitivity and resolution is similar across a wide range of retinal eccentricities when stimulus dimensions are scaled according to cortical magnification (Virsu and Rovamo, 1979; Virsu et al., 1987). For example, monocular vernier acuity is roughly the same except for a scale factor proportional to the retinal eccentricity of the stimulus (Levi and Klein, 1985). If we assume that measurement of vertical disparity is subject to the same scaling, then $\hat{V}SR$ would have approximately equal uncertainty in Ogle's short and tall displays.

In our Experiment 5, stimuli contained 70–400 dots. We know from the control experiment that adding more dots would have little or no effect on slant settings. Thus, as stimulus height was increased, the dots in the display stimulated progressively larger regions of the retina from which the vertical disparities could be measured. Perhaps this allows a more reliable estimate of VSR and, therefore, led to greater reliance on slant estimation by HSR and VSR with increasing stimulus height. Thus, the differences in results between our Experiment 5 and Ogle (1939a) may have been caused by the presence or absence of texture elements between the center and the top and bottom of the stimulus.

8.8. Eccentric location and slant have similar effects on horizontal disparity

In Experiments 2 and 5, we presented images that were consistent with a plane at one azimuth (the VSR azimuth) when the eyes were positioned at a different azimuth. We found that the percept was determined primarily by the azimuth specified by the images, and

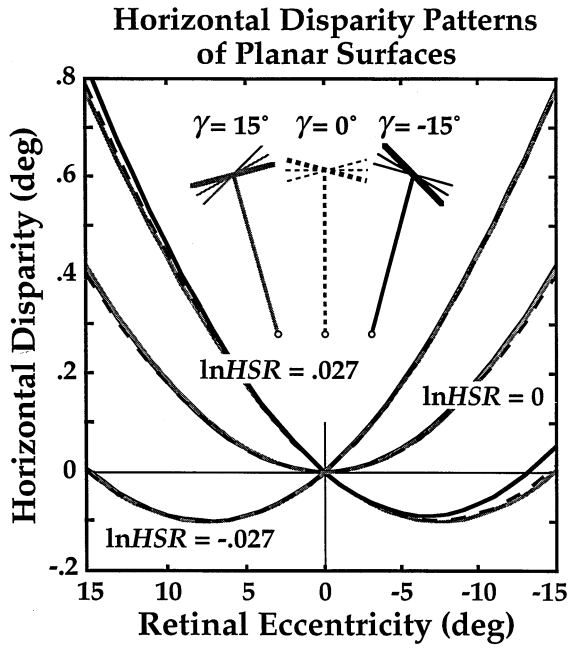

Fig. 22. Horizontal disparity as a function of retinal eccentricity for surfaces of different slants and azimuths. Horizontal disparity (not HSR) is plotted as a function of cyclopean horizontal retinal eccentricity for nine surfaces. The surfaces are positioned at azimuths (γ) of -15, 0, and 15° and slanted such that they give rise to lnHSR values of -0.027, 0, and 0.027. The plan-view icons at the top of the figure represent the azimuths and slants; the thick segments represent patches for which lnHSR = 0.027. The gray curves represent the horizontal disparities for surfaces at an azimuth of 15°. The black dashed curves represent the disparities at an azimuth of 0°. The black solid curves represent the disparities at an azimuth of -15°. The viewing distance used in the calculations for lnHSR values of 0.027 and 0 is 57.3 cm. For lnHSR = -0.027, the viewing distances were 65, 59, and 57.3 cm at $\gamma = 15$, $\gamma = 0$, and $\gamma = -15$°, respectively; the corresponding slants are 30, 15, and 0°.

we attributed this to the vertical disparities within the images. Direct manipulation of vertical disparities in Experiment 3 yielded results consistent with this interpretation. Nonetheless, it is conceivable that the horizontal disparities contained cues to azimuth that were used by the observers. Here we examine this possibility by comparing the patterns of horizontal disparity in the visual plane for planar stimuli presented at different azimuths.

Fig. 22 shows horizontal disparity as a function of retinal eccentricity for nine stimuli. The azimuths of the stimuli are 15, 0, and -15° and the slants are those that give rise to lnHSR values of 0.027, 0, and -0.027. For example, the slants of three surfaces for which lnHSR = 0.027 are: $S = 0$° at $\gamma = 15$°, $S = -14.5$ at $\gamma = 0$, and $S = -28.1$ at $\gamma = -15$. The patterns of horizontal disparities are very similar for the surfaces that give rise to the same value of lnHSR. They can be made nearly identical by small changes in viewing distance (as shown for lnHSR = -0.027; see figure caption). The reason is as follows. When the stimulus is

a plane, the pattern of horizontal disparity (δ) as a function of cyclopean horizontal eccentricity (e) is well-approximated at viewing distances greater than 15 cm by:

$$\delta(e) \approx \tan^{-1}\left(\frac{I}{2d_N}\right)[\cos(\gamma - S) - \cos(2e + \gamma - S)] \qquad (5)$$

where $S - 90 \leq e \leq S + 90$, I is interocular distance, and d_N is the distance between the cyclopean eye and the nearest point on the plane. Thus, the pattern of horizontal disparities is equal for different viewing situations in which d_N and $\gamma - S$ are equal; the disparity pattern of a plane can be matched by another plane at another azimuth by an appropriate choice of distance and slant. As a consequence, observers in our experiments should not have been able to determine surface slant from horizontal disparities alone. Given this, our conclusion from Experiments 4 and 5—that slant perception is based on horizontal disparities and eye position when vertical disparities are rendered unmeasurable—is justified. The analysis portrayed in Fig. 22 also shows that one can characterize the overall pattern of horizontal disparity by a single parameter, as we have done by using the value of lnHSR at fixation.

8.9. Recovery of slant away from fixation

Because HSR and VSR are defined relative to the visual plane, the slant equations presented in Section 1 (Eq. (1)–Eq. (4)) are valid at fixation even when the eyes are directed to the side and upward or downward. In normal viewing, the horizontal meridians of the eyes lie in or nearly in the visual plane because torsion eye movements help align the eyes' images (Rogers, 1992). With such alignment, HSR and VSR can be measured along the eyes' horizontal and vertical meridia.

These equations (Eq. (1)–Eq. (4)) can also be used to recover surface slant at any point in the visual field if the signals are defined properly. Extension to a nonfixated point in the visual plane is straight-forward. Let μ and γ be the vergence and version of the point relative to the head. They can be estimated from felt eye position and the eccentricities of the retinal images. HSR is defined as before. For VSR, the vertical angles β_L and β_R (Fig. 1) must be measured along a great circle in each eye. Thus, a retinal co-ordinate system such as the Fick system (Howard and Rogers, 1995) allows the extension of Eq. (1)–Eq. (4) to non-fixated patches in the visual plane.

The slant estimation equations can also be extended to patches above and below the visual plane. The vertical slant axis must be defined as the line that passes through the center of the patch and is perpendicular to the epipolar plane (i.e. the plane that passes through the patch center and the optical centers of the two eyes). The objective gaze-normal plane is perpendicular to the cyclopean line to the center of the patch and contains the vertical slant axis. Thus, slant becomes the amount by which the patch is rotated about the vertical axis away from the gaze normal. The definitions of μ and γ must be generalized so that they specify location within the epipolar plane; they can again be estimated in principle from felt eye position and the eccentricities of the retinal images. To determine HSR, the horizontal angles α_L and α_R (Fig. 1) must be measured along the great circles in each eye defined by the epipolar plane. For VSR, the vertical angles β_L and β_R must be measured along great circles perpendicular to the epipolar plane. It is not known whether the visual system does this; the point is that the slant equations presented here can in principle be generalized to nonfixated patches above and below the plane of fixation.

8.10. Oblique slants

Our discussion has focused on the estimation of surface slant about a vertical axis. Thus, the only tilts considered were 0 and 180°. (Tilt is defined as a rotation about the line of sight—a surface slanted right side far has 0 tilt, and a surface inclined top far has a tilt of 90°; Stevens, 1983). Naturally, the visual system must estimate both slant and tilt. Here we consider the utility of the slant estimation equations for tilts of different values. The ideas presented here show that even for oblique slant axes, Eq. (1)–Eq. (4) allow recovery of the component of slant about a vertical axis. We then consider the recovery of slant about other axes.

For stimuli slanted about oblique axes, Eq. (1)–Eq. (4) could in principle allow the recovery of the component of slant about the vertical axis. A fixated, planar surface intersects the visual plane in a line. The problem of estimating the component of slant about a vertical axis reduces to finding the slant of the line intersecting the visual plane. The HSR signal is determined by this line. The signals μ and γ are determined by fixation. After examining a number of viewing situations, we assert without proof that VSR is also virtually unaffected by oblique slant. Thus, Eq. (1)–Eq. (4) can be used to determine the slant of the line where a planar surface intersects the visual plane; this is the component of slant about a vertical axis.

To estimate slant about an oblique axis, one has to measure slant about another axis besides the vertical. This could be done by estimating the slant about a horizontal axis and then combining it with an estimate of slant about a vertical axis. The horizontal axis is defined as the intersection of the visual plane and the gaze-normal plane. The slant about a vertical axis determines a line, l_1, where the surface intersects the visual plane. The slant about a horizontal axis determines a second line, l_2, where the surface intersects the

plane that passes through the cyclopean eye and vertical axis. l_1 and l_2 determine the orientation of the surface in space.

Slant about a horizontal axis creates horizontal shear of one eye's image relative to the other, but horizontal shear disparity can also be caused by torsion (rotation of an eye about the visual axis). Therefore, horizontal shear disparity by itself is insufficient to specify slant about a horizontal axis. As with HSR and the estimation of slant about a vertical axis, the visual system requires more information than horizontal shear disparity to estimate slant about a horizontal axis. There are two signals that could in principle be used. First, the torsion (cyclovergence) of the eyes could be measured directly from eye position signals. An extra-retinal torsion signal does in fact exist, but its gain is rather low (Nakayama and Balliet, 1977). Vertical shear disparity is caused by cyclovergence and not by variations in surface slant, so such disparity could be used in interpreting horizontal shear disparity in a manner analogous to the use of VSR in interpreting HSR Porrill, Mayhew and Frisby (1987), Howard and Kaneko (1994). It would be interesting to determine whether both signals—sensed eye position and vertical shear disparity—are used in estimating slant about a horizontal axis and to determine their relative weights in the final estimate.

8.11. Comparison with curvature findings

Experiment 5 revealed a dramatic shift from reliance on HSR and VSR to reliance on HSR and eye position as display height was reduced. A similar effect of display size was reported for perceived curvature of stereoscopic surfaces (Rogers and Bradshaw, 1995) and for perceived depth (Bradshaw et al., 1996); in both cases, observers' percepts were based more on vertical disparity as stimulus size was increased. A quantitative comparison reveals that our data exhibit more reliance on vertical disparity than Rogers, Bradshaw, and colleagues observed. In their curvature study (Rogers and Bradshaw, 1995), the effect of distance specified by eye position was 30% of the complete-constancy prediction for a 38° display. In the work presented here, the effect of azimuth specified by eye position was only 20% in Experiments 2 and 5 for a 30° display. The effects of vertical disparity in Rogers and Bradshaw's curvature study and in our work were 65% and 88%, respectively. The direction of these differences is opposite the prediction made from the difference in display size because larger displays favored vertical disparity in both studies.

This difference in reliance on vertical disparity may be the consequence of using different displays and observers or the consequence of the differing computations needed to estimate curvature and slant. Without a direct comparison of performance on curvature and slant tasks with the same stimuli and observers, one cannot decide. It is interesting nonetheless to consider how the computations required for estimating curvature differ from those in estimating slant. Five signal combinations can be used to determine, stereoscopically, whether a surface is flat or curved: (1) scaling the horizontal gradient of HSR ($\partial \mathrm{HSR}/\partial\gamma$) for distance by using an estimate of μ obtained from extra-retinal signals; (2) scaling the HSR gradient by using an estimate of μ obtained from $\partial \mathrm{VSR}/\partial\gamma$; (3) estimating local slants at various points on the surface using HSR and eye position, then integrating these across space; (4) doing the same, but using HSR and VSR to estimate the local slants; and (5) testing whether $\mathrm{HSR} = k\mathrm{VSR}^2$ throughout the stimulus (Appendix A). There are two means (1) and (3) that use an estimate of μ obtained from extra-retinal signals, and one (4) that might also; these three could, therefore, contribute to the observed effect of vergence. There are also three methods ((2), (4), and (5)) that use vertical disparity, and, therefore, could contribute to the observed effect of vertical disparity.

8.12. Use of signals in other tasks

The same signals used for estimating slant stereoscopically are needed for other computations. We have already noted that curvature and depth estimation require the same signals. Here we consider the use of μ, γ, HSR, VSR, and $\partial \mathrm{VSR}/\partial\gamma$ for estimating the headcentric azimuth and distance of an object.

Frisby (1984) and Gillam and Lawergren (1983) pointed out that vertical magnification of one eye's image does not yield a change in the apparent visual direction of the stimulus. This is somewhat surprising because the visual system does use vertical magnification to correct for changes in stimulus azimuth during slant estimation. Can one understand the absence of a vertical magnification effect on perceived azimuth from an analysis of the signals involved? A simple method for estimating the azimuth of a fixated stimulus from sensed eye position alone is:

$$Azimuth = \gamma \tag{6}$$

A method based on VSR is:

$$Azimuth \approx \tan^{-1}\left(\frac{\ln \mathrm{VSR}}{\mu}\right) \tag{7}$$

where μ is expressed in radians.

From this, one can see why perceived azimuth might be estimated from eye position alone (Eq. (6)) rather than from VSR and μ (Eq. (7)). If azimuth were estimated using VSR, the estimate would be highly susceptible to errors in the estimate of μ, especially at longer viewing distances.

Now consider distance estimation using the aforementioned signals. We can simplify the situation by considering the case in which $\hat{\gamma} = 0$. In that case,

$$\text{distance} \approx \mathrm{I}/\mu \quad (8)$$

where I is interocular distance. μ can be estimated from vergence, but is also equal (in forward gaze) to $\partial\mathrm{VSR}/\partial\gamma$ (see Appendix A). Presuming that $\partial\mathrm{VSR}/\partial\gamma$ can generally be measured reliably, we predict that perceived distance will be less accurate when the surface provides no $\partial\mathrm{VSR}/\partial\gamma$ signal (e.g. is composed of vertical lines).

9. Conclusion

The slant of a stereoscopic surface cannot be determined from the pattern of horizontal disparities (or HSR) alone. However, there are four other signals that, in appropriate combination with horizontal disparity, allow an unambiguous stereoscopic estimate of slant: the vergence (μ) and version (γ) of the eyes, vertical size ratio (VSR), and the gradient of VSR ($\partial\mathrm{VSR}/\partial\gamma$). In addition, a useful signal is provided by perspective slant cues. The determination of perceived slant can be modeled as a weighted combination of three estimates based on those signals: a perspective estimate, a stereoscopic estimate based on HSR and VSR, and a stereoscopic estimate based on HSR and eye position. The visual system must assign a weight to each slant estimate because the estimates may differ; the more reliable the estimate, the larger the weight. It is frequently not obvious a priori which slant estimate is most reliable in part because reliability changes with viewing distance, surface size, surface texture, eye position, and more. In the experiments reported here, slant from HSR and VSR was placed in conflict with slant from HSR and eye position. We found that the visual system generally gives more weight to the former means of slant estimation. However, when VSR is made difficult to measure by using short stimuli or stimuli composed of vertical lines, the visual system gives more weight to sensed eye position (in particular, to the eyes' version). A model in which the slant percept is a linear combination of the two slant estimates accounted well for the data when perspective cues were uninformative. An ideal slant estimator would use the signals and signal combinations that, given the information they provide and the uncertainties in their measurement, would allow the most accurate slant estimate. We do not know if the human visual system uses an ideal weighting scheme, so it will be of interest in the future to identify situations in which optimal and nonoptimal schemes are used.

Acknowledgements

This work was supported by research grants from AFOSR (93NL366) and NSF (DBS-9309820). Additionally, BTB was supported by NIH (T32 EY0704-18) and RVE was supported by Human Frontier of Science (RG-34/96) and by the Foundation for Life Sciences of the Netherlands Organization for Scientific Research. We thank Sharyn Gillett and Sarah Freeman for participating as observers, Karsten Weber for assistance in software development, and Dave Rehder for assistance in constructing the haploscope.

Appendix A

Here we derive the approximations in Eq. (1)–Eq. (4), and describe their accuracy. The viewing geometry is shown and described in Fig. A1.

Derivation of Eq. (1)–Eq. (4):

For reference, equations (1)–(4), are:

$$S \approx -\tan^{-1}\left(\frac{1}{\mu}\ln\frac{\mathrm{HSR}}{\mathrm{VSR}}\right) \quad (1)$$

$$S \approx -\tan^{-1}\left(\frac{1}{\mu}\ln \mathrm{HSR} - \tan\gamma\right) \quad (2)$$

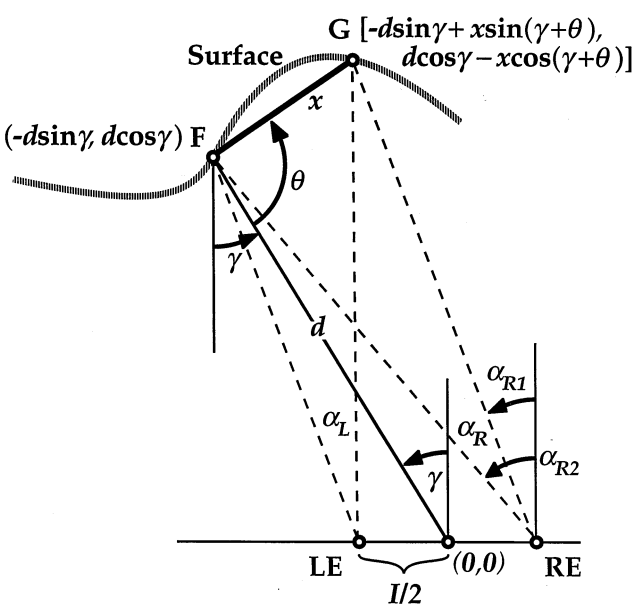

Fig. A1. Quantities used in the derivation of equation Eq. (A3). A smooth surface, represented by the gray curve, is fixated by the two eyes, LE and RE, at point F. The cyclopean eye is at the midpoint between LE and RE and has the co-ordinates (0, 0). The distance, d, to the fixation point is measured along the cyclopean line of sight which is represented by the black diagonal line. The interocular distance is I and the eyes' version is γ. A second point G also lies on the surface and is a distance x from point F. The angles α_L and α_R are the horizontal angles subtended by the surface between F and G at the left and right eyes, respectively. α_{R1} and α_{R2} are the angles formed by a ray pointing straight ahead and the two sides of α_R, so $\alpha_R = \alpha_{R2} - \alpha_{R1}$ (shown); α_{L1} and α_{L2} are similarly defined so $\alpha_L = \alpha_{L2} - \alpha_{L1}$ (not shown). $\theta = S + \pi/2$. The (X, Z) co-ordinates of F and G are shown.

$$S \approx -\tan^{-1}\left(\frac{1}{\tilde{\mu}} \ln \frac{\mathrm{HSR}}{\mathrm{VSR}}\right) \tag{3}$$

$$\tilde{\mu} \approx \frac{1}{2}\left(\frac{\partial \mathrm{VSR}}{\partial \gamma} + \sqrt{(\partial \mathrm{VSR}/\partial \gamma)^2 + 4 \ln(\mathrm{VSR}) \ln(\mathrm{HSR}/\mathrm{VSR})}\right) \tag{4}$$

We begin the derivations by finding HSR at a point F on the surface as an analytic function of S, γ, interocular distance I, and viewing distance d along the cyclopean line of sight. α_L and α_R are the horizontal angles subtended by a surface patch at the left and right eyes, respectively; α_{R1} and α_{R2} are the angles formed by a ray pointing straight ahead and the rays that form the two sides of angle α_R, so $\alpha_R = \alpha_{R2} - \alpha_{R1}$ (shown); α_{L1} and α_{L2} are similarly defined so $\alpha_L = \alpha_{L2} - \alpha_{L1}$ (not shown); $\theta = S + \pi/2$; x is the distance between fixed point F and moveable point G on the surface patch. The ratio $\alpha_L/\alpha_R = \mathrm{HSR}$ is assumed to be differentiable with respect to x at point F. Then:

$$\mathrm{HSR} = \lim_{x \to 0}\left(\frac{\alpha_L}{\alpha_R}\right) = \lim_{x \to 0}\left(\frac{\alpha_{L2} - \alpha_{L1}}{\alpha_{R2} - \alpha_{R1}}\right) \tag{A1}$$

$$= \lim_{x \to 0} \frac{\tan^{-1}\left(\frac{-I/2 + d\sin\gamma}{d\cos\gamma}\right) - \tan^{-1}\left(\frac{-I/2 + d\sin\gamma - x\sin(\gamma+\theta)}{d\cos\gamma - x\cos(\gamma+\theta)}\right)}{\tan^{-1}\left(\frac{I/2 + d\sin\gamma}{d\cos\gamma}\right) - \tan^{-1}\left(\frac{I/2 + d\sin\gamma - x\sin(\gamma+\theta)}{d\cos\gamma - x\cos(\gamma+\theta)}\right)} \tag{A2}$$

L'Hôpital's Rule then yields:

$$\mathrm{HSR} = \left(\frac{d\cos S - (I/2)\sin(\gamma+S)}{d\cos S + (I/2)\sin(\gamma+S)}\right) \cdot \left(\frac{d^2 + dI\sin\gamma + (I/2)^2}{d^2 - dI\sin\gamma + (I/2)^2}\right) \tag{A3}$$

The second factor in Eq. (A3) is equal to the square of the ratio of the distances from F to the right and left eyes, respectively, $(d_R/d_L)^2$, which is also equal to VSR^2, so that:

$$\mathrm{HSR} = \left(\frac{d\cos S - (I/2)\sin(\gamma+S)}{d\cos S + (I/2)\sin(\gamma+S)}\right) \cdot \mathrm{VSR}^2 \tag{A4}$$

Now, at all points on a given line in the visual plane, both $\gamma + S$ and $d\cos S$ are constant as γ varies. It follows that $\mathrm{HSR} = \mathrm{VSR}^2$ for a frontoparallel plane (Rogers and Bradshaw, 1993) and, more generally, that $\mathrm{HSR} = k\mathrm{VSR}^2$ for any plane, where k is the coefficient of VSR^2 in Eq. (A4).

Solving for slant S in Eq. (A4), we obtain the exact relation:

$$S = \tan^{-1}\left(\frac{2d(\mathrm{HSR} - \mathrm{VSR}^2)}{I\cos\gamma(\mathrm{HSR} + \mathrm{VSR}^2)} + \tan\gamma\right) \tag{A5}$$

Equations (1)–(3) follow from Eq. (A5) and from the approximations $\mu \approx I\cos\gamma/d$, $\ln\mathrm{VSR} = \mu\tan\gamma$, $\mathrm{HSR} + \mathrm{VSR}^2 \approx 2$, $\mathrm{HSR} - \mathrm{VSR}^2 \approx \mathrm{HSR} - 2\mathrm{VSR} + 1$, and $\ln(1+\varepsilon) \approx \varepsilon$ for small ε. The expression $\mu \approx I\cos\gamma/d$ has a simple geometrical interpretation. The expression $\ln\mathrm{HSR} \approx \mu\tan\gamma$ can be obtained from the following sequence of approximations:

$$\mathrm{VSR} = \sqrt{\frac{d^2 + dI\sin\gamma + (I/2)^2}{d^2 - dI\sin\gamma + (I/2)^2}} = \sqrt{\frac{1 + \frac{I}{d}\sin\gamma + I^2/4d^2}{1 - \frac{I}{d}\sin\gamma + I^2/4d^2}}$$

Now $d \gg I$ implies

$$\mathrm{VSR} \approx \sqrt{\frac{1 + \frac{1}{d}\sin\gamma}{1 - \frac{1}{d}\sin\gamma}}$$

If either $d \gg I$ or γ is small, we have

$$\mathrm{VSR} \approx 1 + \frac{I}{d}\sin\gamma \tag{A6}$$

Substituting $\mu \approx I\cos\gamma/d$ yields $\mathrm{VSR} \approx 1 + \mu\tan\gamma$ so that $\ln\mathrm{HSR} \approx \mu\tan\gamma$.

Use of the logarithm in Eq. (1)–Eq. (3) yields symmetry in the approximations for S. Consequently, replacing either HSR or VSR with its multiplicative inverse causes only a sign change for the slant estimate. This is exactly what should happen when either $\mathrm{HSR} = 1$, or $\mathrm{VSR} = 1$: S should have the same magnitude, but opposite sign, when the other quantity is replaced with its inverse. It is also approximately what should happen when $\mathrm{HSR} \neq 1$, or $\mathrm{VSR} \neq 1$.

Equation (4) can be derived as follows. As noted above, $d\cos S$ is a constant function of γ, so $\partial(d\cos S)/\partial\gamma = (\partial d/\partial\gamma)\cos S - d\sin S(\partial S/\partial\gamma) = 0$. But $\partial S/\partial\gamma = -1$, so $\partial d/\partial\gamma = -d\tan S$. From the relation $\mathrm{VSR} \approx 1 + (1/d)\sin\gamma$, we obtain:

$$\frac{\partial \mathrm{VSR}}{\partial\gamma} \approx \frac{dI\cos\gamma - I\sin\gamma(\partial d/\partial\gamma)}{d^2} \approx \mu + \frac{I\sin\gamma\tan S}{d}$$

from which

$$\tan S \approx \left(\frac{\partial \mathrm{VSR}}{\partial\gamma} - \mu\right)\frac{d}{I\sin\gamma} \approx \left(\frac{\partial \mathrm{VSR}}{\partial\gamma} - \mu\right)\frac{1}{\ln\mathrm{VSR}}.$$

From Eq. (1), $\tan S \approx -(1/\mu)\ln(\mathrm{HSR}/\mathrm{VSR})$. Equating Eq. (1) and the equation above:

$$\mu^2 - \frac{\partial \mathrm{VSR}}{\partial\gamma}\mu - \ln(\mathrm{VSR})\ln\frac{\mathrm{HSR}}{\mathrm{VSR}} \approx 0 \quad \text{or}$$

$$\mu \approx \frac{1}{2}\left(\frac{\partial \mathrm{VSR}}{\partial\gamma} \pm \sqrt{(\partial \mathrm{VSR}/\partial\gamma)^2 + 4\ln(\mathrm{VSR})\ln(\mathrm{HSR}/\mathrm{VSR})}\right). \tag{A7}$$

There are two solutions to Eq. (A7) which reflects an ambiguity first noted by Longuet-Higgins (1982b). For example, if azimuth γ and slant S are positive, then HSR and $\partial\mathrm{VSR}/\partial\gamma$ are identical to those for another patch on the same VSR curve at azimuth 90-S° with a slant of 90-γ°. Consequently, Eqs. (3) and (4) determine slant from HSR, VSR, and $\partial\mathrm{VSR}/\partial\gamma$ only up to this ambiguity. Recovery of S by means of these equations requires choosing the correct value of $\tilde{\mu}$ from the pair of values represented by the positive and negative roots in Eq. (A7). μ is better estimated by the positive root when $|\gamma + S| < 90°$. This condition is satisfied by all surfaces in forward gaze ($\gamma = 0$), all gaze-normal surfaces when $-90 < \gamma < 90°$, all surfaces for which γ and S are opposite in sign, again when $-90 < \gamma < 90°$, and most surfaces for which γ and S are equal in sign. The positive root is, therefore, given in Eq. (4). Equation (4) reduces to the simple expression:

$$\tilde{\mu} \approx \partial\mathrm{VSR}/\partial\gamma \tag{A8}$$

if either $\mathrm{VSR} = 1$ ($\gamma = 0$), or $\mathrm{HSR} = \mathrm{VSR}$ ($S = 0$).

Other approximations for slant

Mayhew and Longuet-Higgins (1982), provided an approximation for slant in the first half of their equation (19). Expressed in our notation, their equation becomes: $\tan S = -(\mathrm{HSR} - \mathrm{VSR})/(\partial\mathrm{VSR}/\partial\gamma)$, which resembles our Eq. (3), particularly when $\mathrm{VSR} \approx 1$ or $\mathrm{HSR} \approx \mathrm{VSR}$ so that $\tilde{\mu} \approx \partial\mathrm{VSR}/\partial\gamma$.

Another rough, but handy, approximation is:

$$S_{\mathrm{deg}} \approx \gamma_{\mathrm{deg}} - \frac{m \cdot d}{10} \tag{A9}$$

where S and γ are in degrees, m is proximal percent horizontal magnification between the left and right eyes' images ($m = 100 \cdot [\mathrm{HSR} - 1]$), and d is viewing distance in cm.

Accuracy of Eq. (1)–Eq. (4) and Eq. (A9)

Equations (1)–(4) are approximations that represent computations needed to estimate slant stereoscopically. How accurately do they represent the geometry of the binocular viewing situation? To assess their accuracy, we calculated the signals μ, HSR, VSR, and $\partial\mathrm{VSR}/\partial\gamma$, without approximation, for stimuli at various distances, azimuths, and slants; we assumed an interocular distance of 6.0 cm. Equations (1)–(4) were then used to recover slant from these signals and we compared those estimated slants to the actual values.

Slant estimates from Eq. (1) (HSR and VSR) are correct to within 0.002, 0.05, 0.13, and 1.1° of the correct values at viewing distances of 500, 100, 57.3, and 20 cm, respectively, when $-60 \le \gamma \le 60°$ and $-60 \le S \le 60°$. Estimates from Eq. (2) HSR and eye position) are correct to within 0.004, 0.09, 0.25, and 2.1° at the same distances, respectively, for the same ranges of γ and S. As $|\gamma + S|$ approaches 90° from below, Eq. (4) becomes markedly less accurate. For $|\gamma + S| \le 80°$, Eq. (4) estimates μ from HSR, VSR, and $\partial\mathrm{VSR}/\partial\gamma$ to within 5×10^{-5}, 0.006, 0.03, and 0.67°, respectively, of the correct values; for $|\gamma + S| \le 60$, it is accurate to within 2×10^{-5}, 0.002, 0.01, and 0.25°. Slant estimates from Eq. (3) are accurate when $\tilde{\mu}$ (i.e. the estimate of μ from Eq. (4)) is accurate. For $|\gamma + S| < 80$, the equation estimates slant to within 0.004, 0.10, 0.30, and 3.2°, respectively, of the correct values. For $|\gamma + S| < 60$, Eq. (3) is accurate to within 0.002, 0.04, 0.13, and 1.0°, respectively. Finally, if the magnitudes of γ and S are both less than 15°, Eq. (A9) is good to within 2° beyond 57.3 cm, and to within 3° at 20 cm.

References

Ames, A. Jr., Ogle, K. A., & Gliddon, G. H. (1932). Corresponding retinal points, the horopter and size and shape of ocular images. *Journal of the Optical Society of America*, *22*, 538–575.

Amigo, G. (1967). The stereoscopic frame of reference in asymmetric convergence of the eyes. *Vision Research*, *7*, 785–799.

Amigo, G. (1972). The stereoscopic frame of reference in asymmetric convergence of the eyes: response to point stimulation of the retina. *Optica Acta*, *19*, 993–1006.

Banks, M. S., & Backus, B. T. (1998). Extra-retinal and perspective cues cause the small range of the induced effect. *Vision Research*, *38*, 187–194.

Bishop, P. O. (1994). Size constancy, depth constancy and vertical disparities: a further quantitative interpretation. *Biological Cybernetics*, *71*, 37–47.

Bishop, P. O. (1996). Stereoscopic depth perception and vertical disparity: neural mechanisms. *Vision Research*, *36*, 1969–1972.

Bradshaw, M. F., Glennerster, A., & Rogers, B. J. (1996). The effect of display size on disparity scaling from differential perspective and vergence cues. *Vision Research*, *36*, 1255–1264.

Braunstein, M. L. (1968). Motion and texture as sources of slant information. *Journal of Experimental Psychology*, *78*, 247–253.

Buckley, D., & Frisby, J. P. (1993). Interaction of stereo, texture and outline cues in the shape perception of three-dimensional ridges. *Vision Research*, *33*, 919–933.

Clark, F. J., Horch, K. W. (1986). Kinesthesia. In: K. R. Boff, L. Kaufman, J. P. Thomas, *Handbook of perception and human performance*, *vol. I*, *Sensory processes and perception*. New York: John Wiley and Sons.

Collett, T. S., Schwarz, U., & Sobel, E. C. (1991). The interaction of oculomotor cues and stimulus size in stereoscopic depth constancy. *Perception*, *20*, 733–754.

Cumming, B. G., Johnston, E. B., & Parker, A. J. (1991). Vertical disparities and the perception of three-dimensional shape. *Nature*, *349*, 411–413.

Cumming, B. G., Johnston, E. B., & Parker, A. J. (1993). Effects of different texture cues on curved surfaces viewed stereoscopically. *Vision Research*, *33*, 827–838.

Cutting, J. E., & Millard, R. T. (1984). Three gradients and the perception of flat and curved surfaces. *Journal of Experimental Psychology*: *General*, *113*, 198–216.

Ebenholtz, S. M., & Paap, K. R. (1973). The constancy of object orientation: compensation for ocular rotation. *Perception and Psychophysics*, *14*, 458–470.

Erkelens, C. J., van Ee, R. (1998). A computational model of depth perception based on headcentric disparity. *Vision Research*, (in press).

Foley, J. M. (1980). Binocular distance perception. *Psychological Review*, *87*, 411–434.

Frisby, J. P. (1984). An old illusion and a new theory of stereoscopic depth perception. *Nature*, *307*, 592–593.

Gårding, J., Porrill, J., Mayhew, J. E., & Frisby, J. P. (1995). Stereopsis, vertical disparity and relief transformations. *Vision Research*, *35*, 703–722.

Gillam, B., & Lawergren, B. (1983). The induced effect, vertical disparity, and stereoscopic theory. *Perception and Psychophysics*, *34*, 121–130.

Gillam, B., & Ryan, C. (1992). Perspective, orientation disparity, and anisotropy in stereoscopic slant perception. *Perception*, *21*, 427–439.

Gillam, B., Chambers, D., & Lawergren, B. (1988). The role of vertical disparity in the scaling of stereoscopic depth perception: an empirical and theoretical study. *Perception and Psychophysics*, *44*, 473–483.

Green, J. (1889). On certain stereoscopical illusions evoked by prismatic and cylindrical spectacle-glasses. *Transactions of the American Ophthalmology Society*, 449–456.

Heller, L. M., & Trahiotis, C. (1996). Extents of laterality and binaural interference effects. *Journal of the Acoustical Society of America*, *99*, 3632–3637.

Herzau, W., & Ogle, K. N. (1937). Über den Grössenunterschied der Bilder beider Augen bei asymmetrischer Konvergenz und seine Bedeutung für das Zweiäugige Sehen. *Albrecht von Graefes Archiv für Ophthalmologie*, *137*, 327–363.

Howard, I. P., & Kaneko, H. (1994). Relative shear disparities and the perception of surface inclination. *Vision Research*, *34*, 2505–2517.

Howard, I. P., Rogers, B. J. (1995). Binocular vision and stereopsis. Oxford, New York.

Klein, S. A., Hu, Q. J., & Carney, T. (1996). The adjacent pixel nonlinearity: problems and solutions. *Vision Research*, *36*, 3167–3181.

Koenderink, J. J., & van Doorn, A. J. (1975). Invariant properties of the motion parallax field due to the movement of rigid bodies relative to an observer. *Optica Acta*, *22*, 773–791.

Koenderink, J. J., van Doorn, A. J. (1976). Geometry of binocular vision and a model for stereopsis. *Biological Cybernetics*, *21*, 2129–2135.

Landy, M. S., Maloney, L. T., Johnston, E. B., & Young, M. (1995). Measurement and modeling of depth cue combination: in defense of weak fusion. *Vision Research*, *35*, 389–412.

Levi, D. M., & Klein, S. A. (1985). Vernier acuity, crowding and amblyopia. *Vision Research*, *25*, 979–991.

Lippincott, J. A. (1889). On the binocular metamorphopsia produced by correcting glasses. *AMA Archives of Ophthalmology*, *18*, 18–30.

Longuet-Higgins, H. C., & Prazdny, K. (1980). The interpretation of a moving retinal image. *Proceedings of the Royal Society of Lond* [*Biology*], *208*, 385–397.

Longuet-Higgins, H. C. (1982a). The role of the vertical dimension in stereoscopic vision. *Perception*, *11*, 377–386.

Longuet-Higgins, H. C. (1982b). Appendix to paper by John Mayhew entitled: the interpretation of stereo-disparity information: the computation of surface orientations and depth. *Perception*, *11*, 405–407.

Mayhew, J. E. W., & Longuet-Higgins, H. C. (1982). A computational model of binocular depth perception. *Nature*, *297*, 376–378.

Mayhew, J. E. W. (1982). The interpretation of stereo–disparity information: the computation of surface orientation and depth. *Perception*, *11*, 387–403.

Nakayama, K., & Balliet, R. (1977). Listing's law, eye position sense, and perception of the vertical. *Vision Research*, *17*, 453–457.

Ogle, K. N. (1938). Induced size effect. I. A new phenomenon in binocular space-perception associated with the relative sizes of the images of the two eyes. *Archives of Ophthalmology*, *20*, 604–623.

Ogle, K. N. (1939a). Induced size effect. II. An experimental study of the phenomenon with restricted fusion stimuli. *Archives of Ophthalmology*, *21*, 604–625.

Ogle, K. N. (1939b). Relative sizes of ocular images of the two eyes in asymmetric convergence. *Archives of Ophthalmology*, *22*, 1046–1067.

Ogle, K. N. (1940). Induced size effect with the eyes in asymmetric convergence. *Archives of Ophthalmology*, *23*, 1023–1028.

Ogle, K. N. (1950). Researches in binocular vision. W.B. Saunders: Philadelphia, London.

Porrill, J., Mayhew, J. E. W. & Frisby, J. P. (1987). Cyclotorsion, conformal invariance and induced effects in stereoscopic vision. In: *Frontiers of visual science: Proceedings of the 1985 Symposium*. Washington, D.C.: National Academy Press.

Rogers, B. J., & Bradshaw, M. F. (1993). Vertical disparities, differential perspective and binocular stereopsis. *Nature*, *361*, 253–255.

Rogers, B., & Bradshaw, M. (1995). Disparity scaling and the perception of frontoparallel surfaces. *Perception*, *24*, 155–179.

Rogers, B. J. (1992). The perception and representation of depth and slant in stereoscopic surfaces. In G. Orban, & H. Nagel, *Artificial and biological vision systems*. Berlin: Springer, 241–266.

Rosenholtz, R., & Malik, J. (1997). Surface orientation from texture: isotropy or homogeneity or both? *Vision Research*, *37*, 2283–2293.

Schor, C. M., Maxwell, J. S., & Stevenson, S. B. (1994). Isovergence surfaces: the conjugacy of vertical eye movements in tertiary positions of gaze. *Ophthalmic and Physiological Optics*, *14*, 279–286.

Sedgwick, H. (1986). Space perception. In K. R. Boff, L. Kaufman, & J. P. Thomas, *Handbook of perception and human performance*. In: *Sensory processes and perception*, Vol. I. New York: John Wiley and Sons.

Sobel, E. C., & Collett, T. S. (1991). Does vertical disparity scale the perception of stereoscopic depth? *Proceedings of the Royal Society of London* [*Biology*], *244*, 87–90.

Stevens, K. A. (1981). The information content of texture gradients. *Biological Cybernetics*, *42*, 95–105.

Stevens, K. A. (1983). Slant-tilt: the visual encoding of surface orientation. *Biological Cybernetics*, *46*, 183–195.

van Ee, R., & Erkelens, C. J. (1996). Stability of binocular depth perception with moving head and eyes. *Vision Research*, *36*, 3827–3842.

Virsu, V., & Rovamo, J. (1979). Visual resolution, contrast sensitivity, and the cortical magnification factor. *Experimental Brain Research*, *37*, 475–494.

Virsu, V., Näsänen, R., & Osmoviita, K. (1987). Cortical magnification and peripheral vision. *Journal of the Optical Society of America A*, *4*, 1568–1573.

von Helmholtz, H. (1962). Physiological Optics J.P.C. Southall for the Optical Society of America 1924, Translated. New York: Dover.